AN ABSTRACT OF THE THESIS OF

Gregory Leonard Will for the degree M.S.

in Agricultural Engineering presented on December 12, 1973

Title: Infiltration Under a Rainfall Simulator

Abstract approved: Redacted for privacy

Royal H. Brooks

A large rainfall simulator was used to study infiltration on six soil plots. Water content and capillary pressure were measured during steady rainfall at rates less than required to produce runoff. The equipment and procedures used to make these measurements are discussed. Water content and capillary pressure data obtained as a function of time were combined to produce the *in situ* water holding capacity curve for the profile. The results were compared with data obtained from soil samples using conventional laboratory techniques.

Infiltration capacity curves were also obtained for these soils using high rates of rainfall. The infiltration capacity curves for the plots are compared using scaled variables.

Infiltration Under a Rainfall Simulator

by

Gregory Leonard Will

A THESIS

submitted to

Oregon State University

in partial fulfillment of
the requirements for the
degree of

Master of Science

Completed December 12, 1973

Commencement June 1974

APPROVED:

Redacted for privacy

Associate Professor of Agricultural Engineering
in charge of major

Redacted for privacy

Head of Department of Agricultural Engineering

Redacted for privacy

Dean of Graduate School

Date thesis is presented December 12, 1973

Typed by Silvily Sandstrom for Gregory Leonard Will

ACKNOWLEDGEMENTS

The research for this thesis was carried out in partial fulfillment of the requirements for a Masters degree in Agricultural Engineering at Oregon State University, Corvallis, Oregon. This work was performed under a cooperative agreement with the Agricultural Research Service, Northwest Watershed Research Center, Boise, Idaho, and Oregon State University (agreement No. 12-14-100-5363(41).

The author wishes to acknowledge with gratitude the contributions of his advisor, Dr. Royal H. Brooks. The encouragement and advice during the various stages of the research program and particularly in the preparation of this thesis are greatly appreciated.

Personal gratitude is expressed to Michael J. McLatchy and Walter J. Rawls for their help in obtaining the field data.

The high quality work of the people who assisted in putting this thesis together is gratefully acknowledged. Special thanks are extended to Silvily Sandstrom for a fine job of typing and to Pete Lyngstrand for his excellent draftsmanship.

Finally, the author is deeply appreciative for the encouragement and assistance of his wife, Elizabeth. Without her understanding patience, the author could not have met the requirements for this degree.

TABLE OF CONTENTS

LIST OF ILLUSTRATIONS

LIST OF TABLES

LIST OF SYMBOLS

a	Coefficient in imbibition equation.
b	Coefficient in imbibition equation.
g	Acceleration of gravity.
k	Permeability.
K	Conductivity.
P_c	Capillary pressure.
P_b	Bubbling pressure.
$P.$	Scaled pressure.
S	Saturation.
S_r	Residual Saturation.
$S.$	Scaled saturation.
t	Time.
$t.$	Scaled time.
λ	Pore-size distribution index.
μ	Absolute viscosity.
ρ	Density.
ϕ_e	Effective porosity.

INFILTRATION UNDER A RAINFALL SIMULATOR

I. INTRODUCTION

As more and more hydraulic structures are being built, it becomes increasingly vital to be able to make accurate predictions of infiltration and runoff. The use of these predictions range from flood control and reservoir regulation to predicting the amount of water available throughout the year for hydroelectric power and irrigation. Another important use is to help determine the size of hydraulic structures needed to handle the runoff yield a certain watershed can produce.

Watershed models or emperical equations are often used for predicting the various aspects of watershed hydrology. Generally these methods have required a great deal of previous rainfall and runoff data from the watershed of interest. These methods can usually be used on well gauged watersheds but can rarely be used on ungauged watersheds.

Need for Study

The need for predictions on ungauged watersheds has led investigators to study in detail the various aspects of runoff and infiltration. Some investigators have used these studies to construct mathematical models from basic properties of the watershed. Infiltration is probably the most important but the least understood aspect of watershed hydrology.

Rainfall simulators or infiltrometers have been used to study infiltration and may provide useful information needed to construct

mathematical or emperical predictive schemes. This is especially true if the infiltration process is well documented both above and below the soil surface to give a total view of water movement.

Objectives of Study

The objectives formulated to contribute to the above need were to instrument and study water movement under a large rainfall simulator-infiltrometer and to determine the practicality of using this equipment to characterize watershed soils.

Considerable time was spent developing techniques and instrumentation before going to the field. During the summer of 1972, the Agricultural Research Service of the Northwest Watershed Research Center, Oregon State University, and Utah State University placed a team of individuals into the field with instrumentation, rainfall simulator-infiltrometer, and supporting equipment for the purpose of satisfying the above objectives.

II. BACKGROUND AND REVIEW OF LITERATURE

Various types of infiltrometers have been used to determine the infiltration capacity of soils. These infiltrometers fall into two general classes: (1) those in which the rate of intake is determined directly by the rate at which water must be added to maintain a constant depth within the infiltrometer and (2) rainfall simulators.

Ring Infiltrometers

Burgy and Luthin (1956) ran field experiments on single and double ring infiltrometers which fall into the first class. They found that on a uniform soil profile having no layers restricting the downward movement of water, that six infiltrometer measurements per area gave an average figure that was within 30 percent of the true mean obtained by flooding each area. There were no significant differences in the results obtained with the two types of infiltrometers.

Shull (1964) investigated the effect of installation depth on infiltration rates obtained from single ring infiltrometers. He found that the depth of installation had a significant effect on the infiltration rates.

Although this first class of infiltrometers gives a simple and direct method of determining infiltration rates, the results are good only for qualitative comparisons. The reasons for this, given by Wisler and Brater (1967) are: (1) the effect of the beating of raindrops, with the resulting compaction and inwash of fine materials, is absent; (2) the effect of compression of the entrapped air is absent because of lateral escape; (3) it is impossible to place a ring or

tube in the ground without disturbing the soil structure near the boundary.

Rainfall Simulators

In order to eliminate the above disadvantages, various infiltrometers have been used which sprinkle water on a plot in excess of the infiltration rate and collect the runoff.

Wilm (1941) ran field experiments with four types of rainfall simulators. They were: (1) Type-F infiltrometer, modified (measuring 6.6 feet by 12 feet), (2) Rocky Mountain infiltrometer (2 feet by 4 feet), (3) Modified North Fork (2.5 square feet) and (4) Pearse square-foot (1 foot square). The data demonstrates that infiltration rates are characteristically variable. The largest part of variation occurs between sites in a single plant-type and smaller amount of variation may be due to errors of instruments and technique. Any of the four infiltrometers can be expected to give only relative estimates of true infiltration. The Type-F instrument gave results higher than with the smaller three instruments, which agreed relatively well among themselves. Any of the four should give satisfactory estimates of relative infiltration rates.

Effect of Soil Properties on Infiltration

There are many factors which affect infiltration. A factor Colman and Bodman (1945) studied experimentally was the effect of texturally layered soil profiles. They found in layered columns that the less permeable layer limited infiltration regardless of its position in the soil profile. Hank's and Bower's (1962) solutions obtained

for infiltration into a loam over a silt loam and vice versa followed the earlier results providing the wetting front had extended well into the second layer. Miller and Bunger (1963) showed that a soil underlaid by sand or gravel retained more moisture than when the soil was uniform throughout the profile.

Various other factors such as vegetative cover, freezing effects and soil macrostructure are discussed in Wisler and Brater (1967).

III. METHODS AND PROCEDURES

Field Equipment

The field data was obtained from Reynolds Creek Experimental Watershed in southwest Idaho shown in Figure 1 and described by Robins, Kelly, and Hamon (1965). Experiments were run on six plots at three different areas within the 90 square mile watershed. The data was obtained from a specially designed rainfall simulator equipped with sensors for measuring infiltration as shown in Figure 2 and described by Penton and Hammon (in press). The simulator was accompanied by a camper used as an instrument shelter, a 110 volt ac electrical generator as shown in Figure 3, and a water supply tank.

Rainfall Simulator

The rainfall simulator, Figure 4, is portable and consists of (1) a pipe-frame stand, (2) six rain producing modules, (3) an air blower, and (4) controls for air pressure and water flow rate regulation as shown in a close-up in Figure 5. The pipe-frame stand can be adjusted to any grade from 0-100 percent so that the rain producing modules may be maintained in a level position. On level ground, the six rain producing modules are eight feet above the soil surface. Rainfall intensities can be varied from 1.27 cm to 20.3 cm/hr. The drop size can be varied from 0.2 mm to 3.7 mm by adjusting the air pressure in the module duct system.

Gamma Probe

To monitor the water movement in the soil, a Troxler Model 2376 two-probe gamma density meter was used. This instrument consisted of

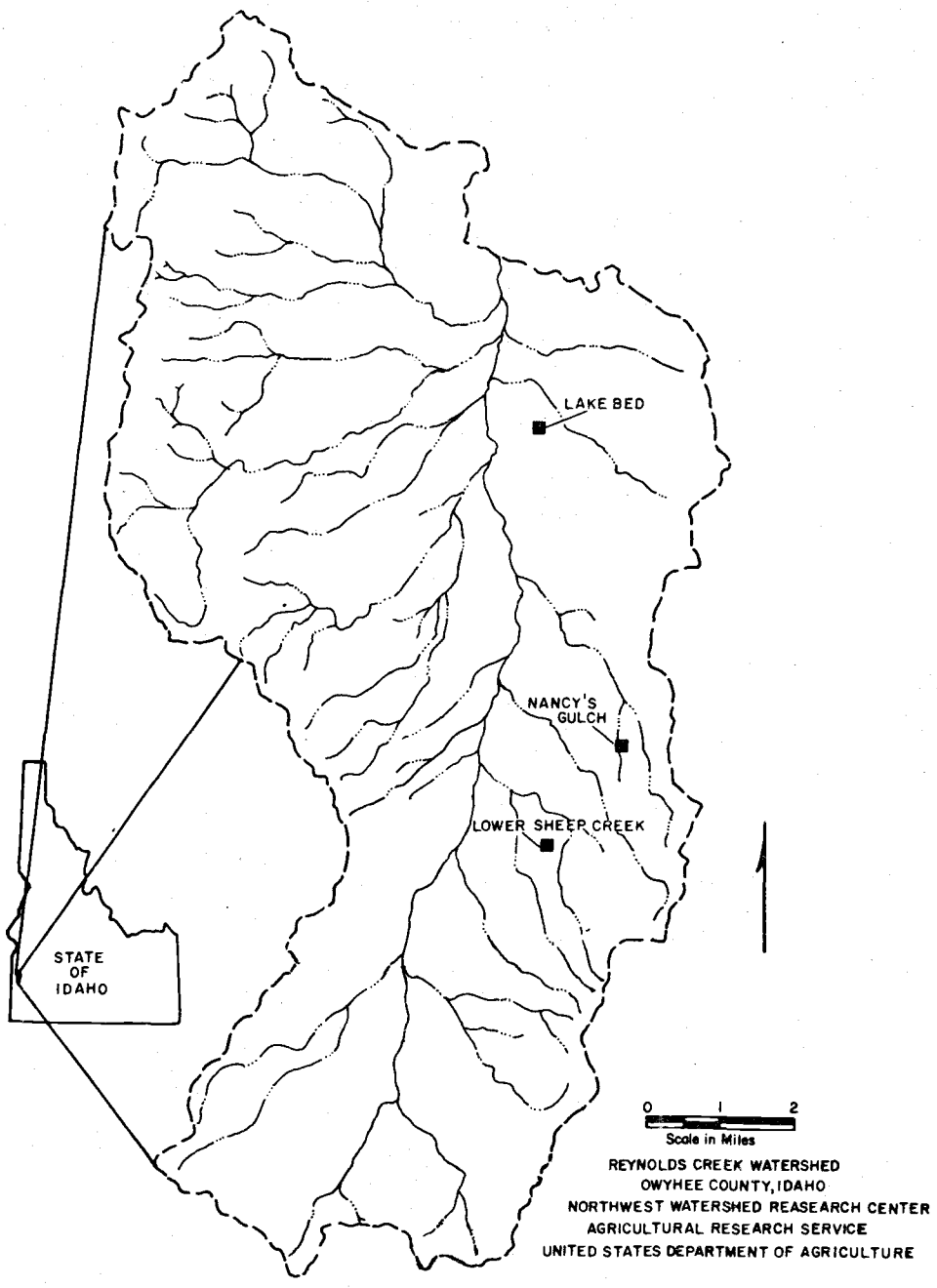

Figure 1. Map of Reynolds Creek Watershed and location of infiltration plots.

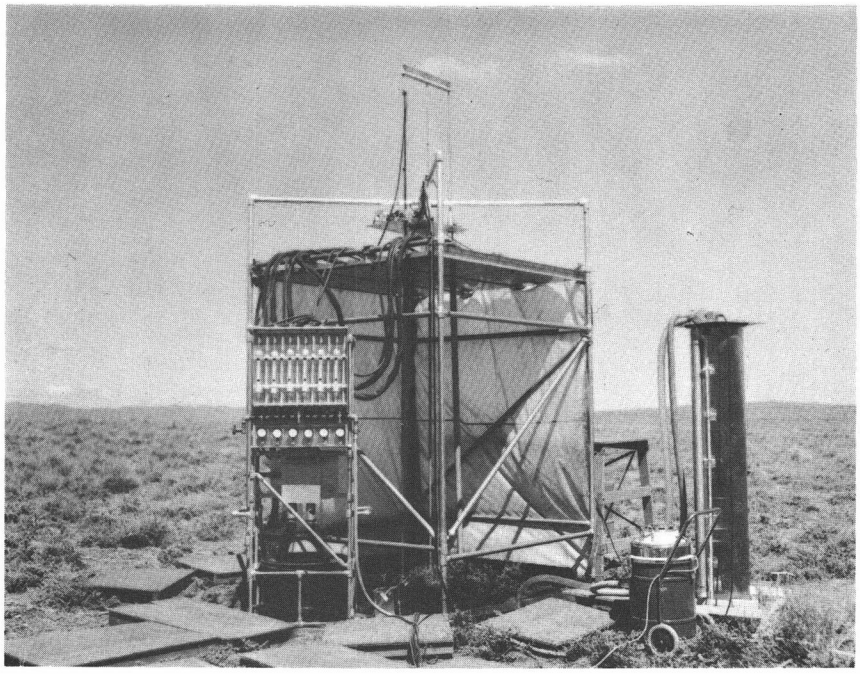

Figure 2. Picture of rainfall simulator with part of curtain removed, and runoff measuring tank on the right.

Figure 3. Picture of rainfall simulator, camper for housing instrumentation, and electrical generator which supplied all electrical power.

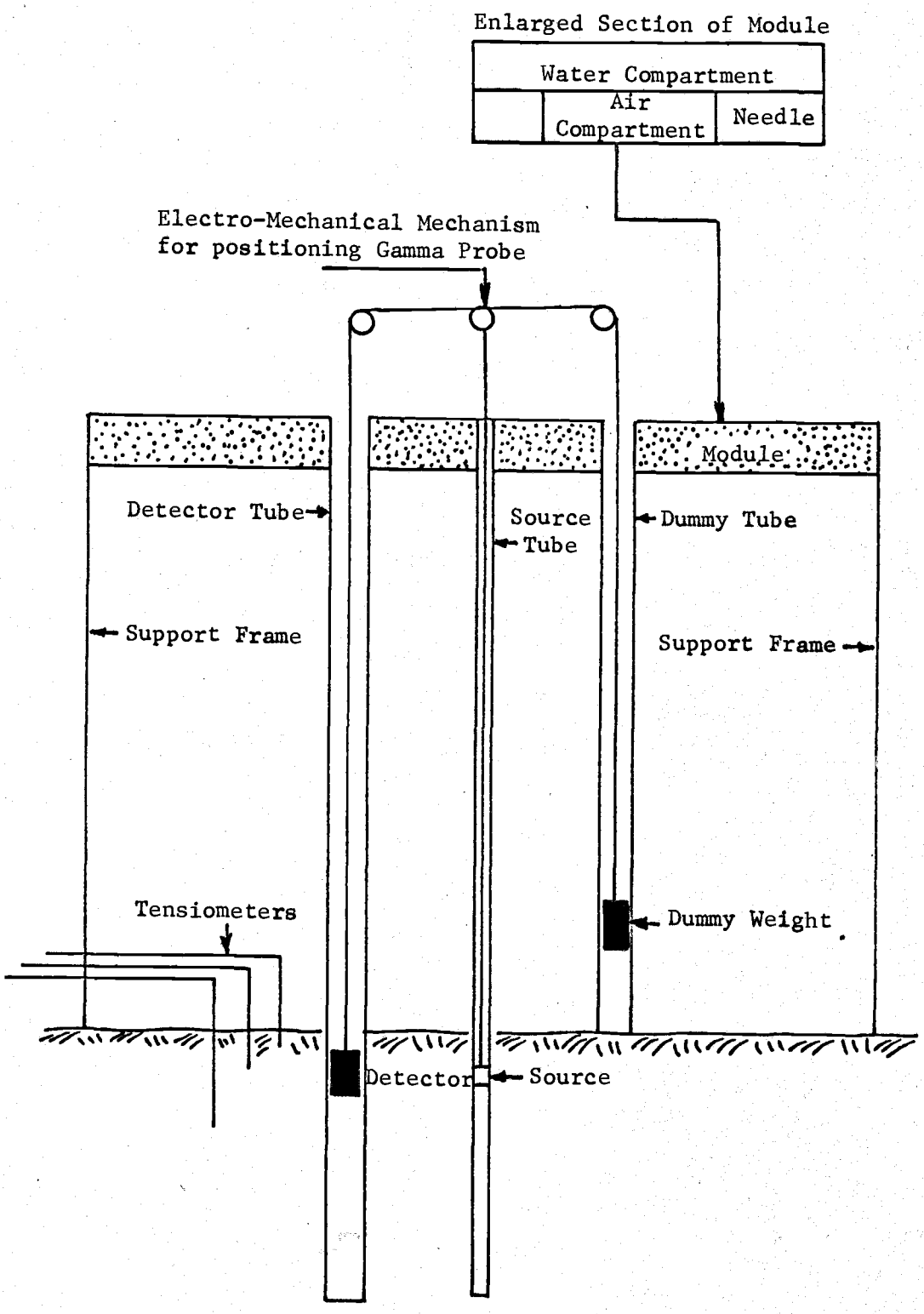

Figure 4. Schematic diagram of rainfall simulator showing sensors for capillary pressure and saturation.

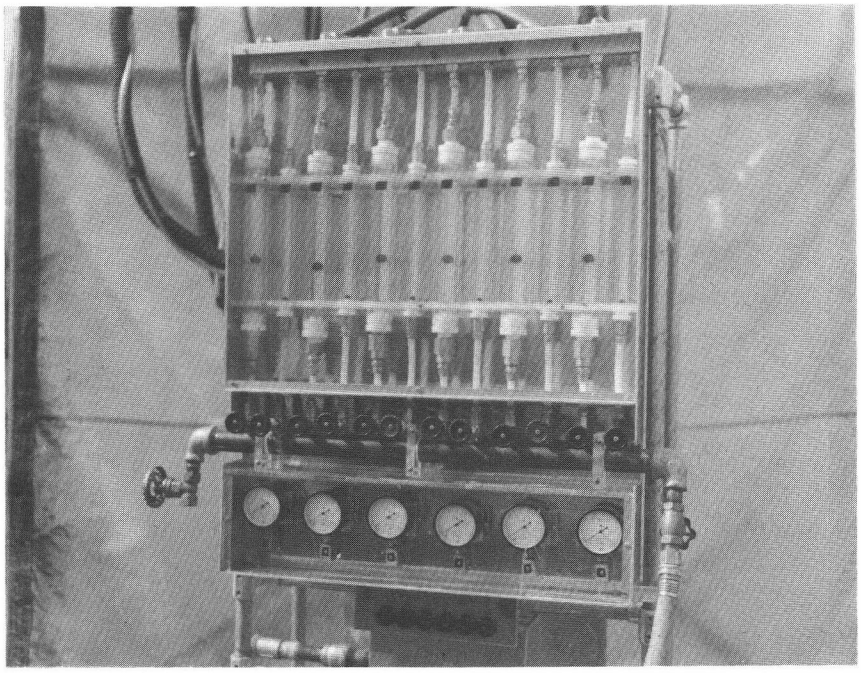

Figure 5. Picture of water flow regulating valves and flow meters for the six rainfall modules (top) and air pressure regulating valves and pressure gauges (bottom).

Figure 6. Picture showing an infiltration plot with vertical access tubes for gamma probe and source (see Fig. 4), three tensiometers with nylon tubing going to insulated pressure transducer box, steel border around plot, typical vegetative cover, and pipe frame stand.

(1) a source probe, (2) a detector probe, and (3) a gamma counter-rate meter. Two test holes, 12 inches apart, were required at each site for the two probes shown in Figures 4 and 6. A third hole was present at most of the sites and was used for a counterweight, but was unnecessary. The source probe contained five mCi Cs-137 and was stored in a lead container when not in use. The detector probe, which was always directly opposite from the source probe in Figure 4, picked up the gamma emissions that passed through the 12 inches of soil between the probes. The gamma counter indicated the number of emissions for one minute on a digital display, while the rate meter gave a continuous reading of the intensity of emissions. To measure emissions at different soil depths, the probes were mounted on a mechanism connected to the simulator frame that allowed the probes to be remotely raised and lowered to any depth. By calibrating the gamma system with materials of known density, the gamma counts could be converted to soil densities. As the moisture content of the soil between the probes increased, the number of emissions that hit the detector decreased corresponding to an increase in soil density. These density changes were later correlated with the dry bulk densities of the soil at the corresponding depth to give percent saturation of the soil.

The depth of the probes below the soil surface and gamma emission rate were indicated on a multi-channel strip-chart recorder. A ten-turn potentiometer, driven by the probe drive mechanism converted the position of the mechanism into a voltage output using the circuit in Figure 7.

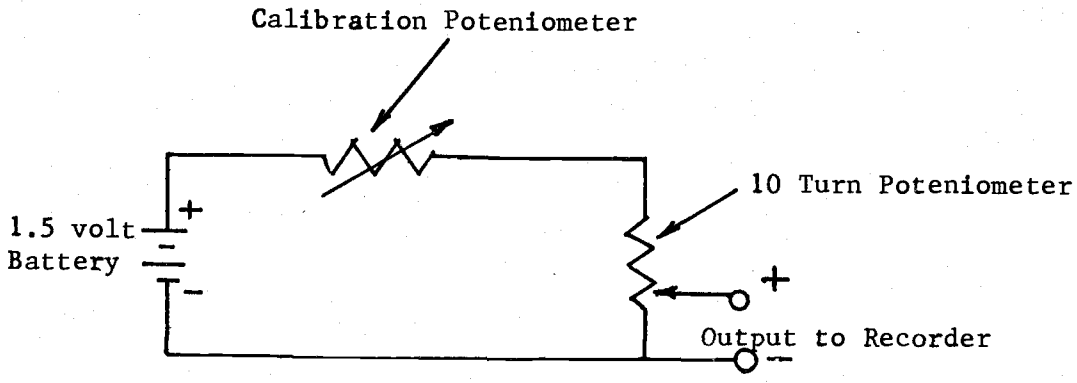

Figure 7. Circuit for converting mechanical position to an electrical output.

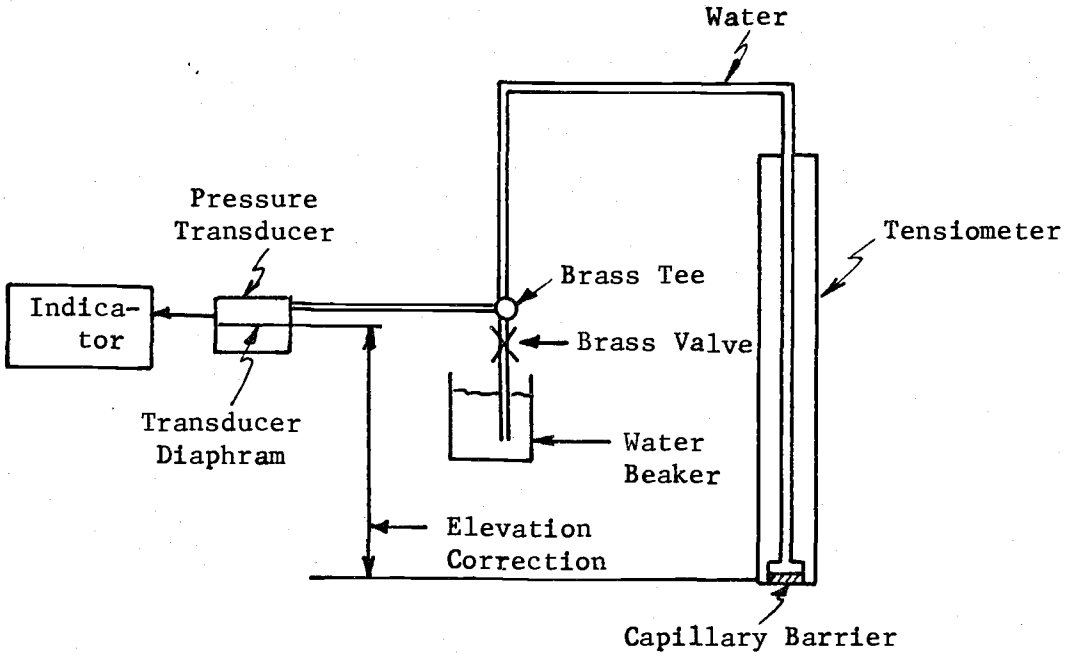

Figure 8. Schematic of the tensiometer-pressure transducer system used to obtain capillary pressure head as a function of saturation data in infiltration plots.

Tensiometers

Capillary pressure was obtained with a tensiometer-pressure transducer system shown in Figure 8. Before the tensiometers could be installed in the field, the pressure transducers had to be calibrated. They were first calibrated in the laboratory using a vacuum pump, a vacuum-pressure regulator, and a U-tube mercury manometer. The tensiometer capillary barriers were vacuum saturated and tested for leaks before going to the field. Before installing at the field, the calibration curve was checked on each transducer by holding the tensiometer capillary barrier at a measured distance below the transducer diaphrams. By checking at three different elevations, the calibration curves could be checked. The tensiometers were installed 5.1, 10.2 and 20.3 cm below the soil surface, close to the gamma probe access tubes. Since the soil tension was very high when tensiometers were first installed, water was added occasionally through the tensiometers by a valve to keep transducers on scale and to prevent breaking the capillary barrier in the tensiometers. The transducers were operated in an insulated box so that temperature variations would not affect them. After data were collected, it had to be corrected to account for the elevation difference between the transducer diaphrams and the tensiometer capillary barriers.

Runoff Collector

At the higher intensities when runoff occurred, a runoff collector was used. It consisted of (1) steel borders shown in Figure 6, installed 25.4 to 30.5 cm deep on three sides of the plot and (2) runoff collecting trough on the downslope side. Water was drawn into a

measuring tank shown in Figure 3 by using an industrial vacuum cleaner. A vacuum was created in the top of the tank which caused the water to be drawn into it. The water level in the tank was monitored using a float and counterweight system. As the float raised in the tank it caused a wheel to turn which was connected to a ten-turn potentiometer in a ciucuit shown in Figure 7. This circuit gave an electrical output which was proportional to the water level in the tank.

All the data that were collected from the experiments were recorded on a multi-channel strip-chart recorder. A block diagram of the electronic instrument and control system is shown in Figure 9.

Field Data Collection

The first experiment on each plot was a low intensity run without steel borders around the plot. Before the rain was turned on, an initial soil density profile was obtained. A series of one minute gamma counts were obtained at different depths, then the profile was scanned continuously at a constant slow rate from the lowest depth. After the initial conditions, the flow meters on the simulator were adjusted for a 1.27 or 1.78 cm/hr rainfall rate. The tensiometers were kept primed until the soil tension at their respective depths came into the tensiometer range. All during the runs, one minute gamma counts were taken at depths where the counts were changing with time. After a series of counts was taken, a scan of that portion of the profile would be taken. From the scans, the approximate depth of the wetting front could be detected from a large change in gamma counts from the previous scan. When the wetting front had reached 30.5 to 38.1 cm the rain would be shut off and a final moisture profile taken using the

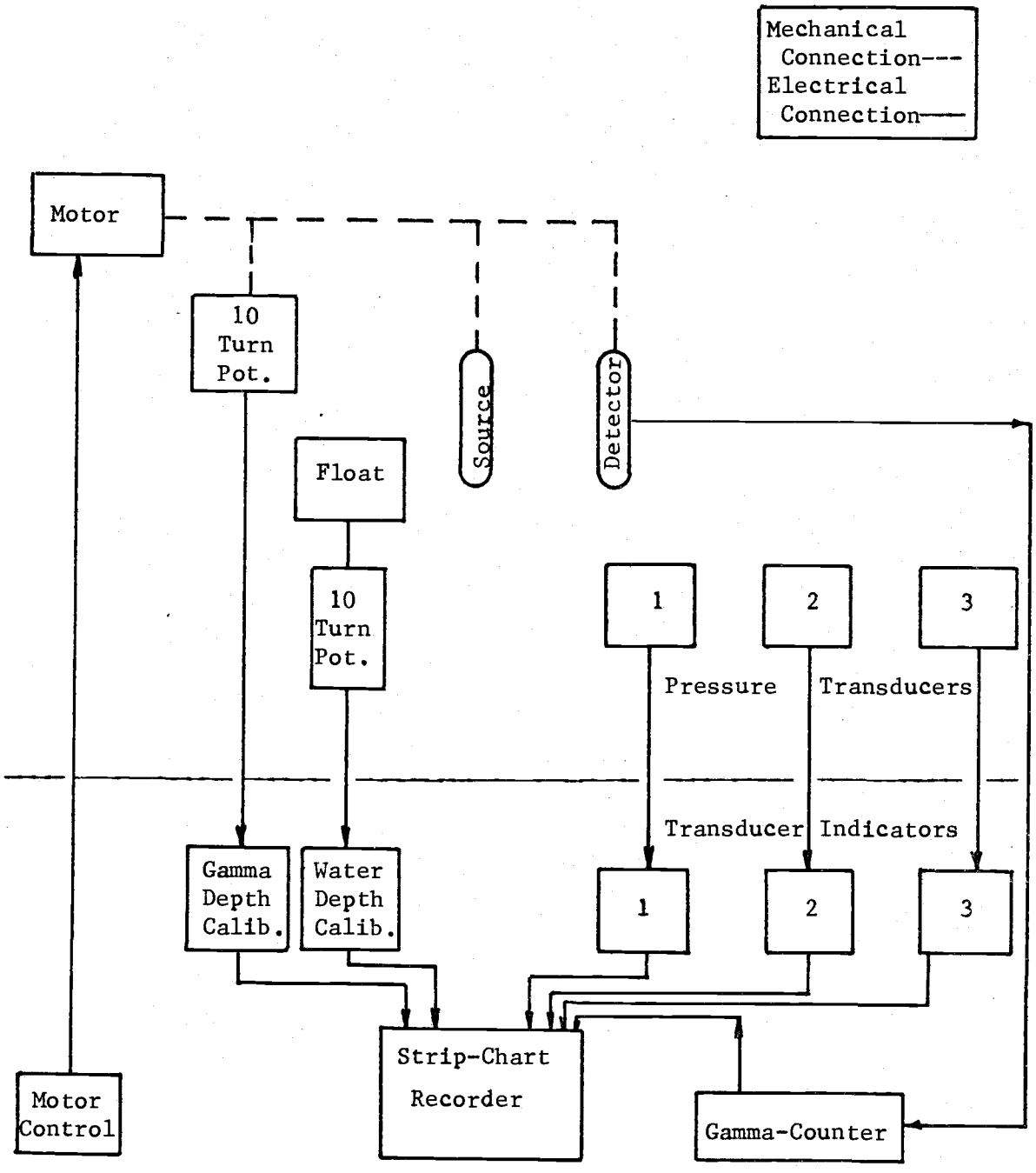

Figure 9. Schematic diagram showing the electrical and mechanical connections of the sensing and recording equipment.

same method as used for the initial profile.

On the first two plots (68057196 and 68057396) at the Lakebed, a second low intensity experiment was run three days after the first low intensity was run. The only difference between the runs was that the second had the steel borders installed to simulate a one-dimensional case. After two plots were run using the second low intensity run, it was decided that for the size of plot used, there was little difference between the experiment with borders and the one without. As a result, the second run was omitted so that data from more plots could be obtained.

A third experiment was run to obtain an infiltration capacity curve. A rainfall rate was used which was in excess of the infiltration rate, usually 5 to 7.6 cm per hour. The runoff was collected and measured. When the runoff rate remained constant for at least half an hour, the experiment was terminated. Since the plots were still quite wet at the beginning of this experiment, little attempt was made to obtain capillary pressure.

Soil Samples and Laboratory Measurements

After the field experiments were run, two inch soil core samples were taken at 5.1, 10.2 and 20.3 cm depths near the gamma probe access tubes at each plot. These samples were taken to the laboratory where pressure-saturation curves were run. A diagram of the apparatus that was used is shown in Figure 10.

The capillary barrier was vacuum saturated with water and tested for leaks. A soil core was then carefully trimmed and placed into the apparatus. The cell was then placed in water until the soil was

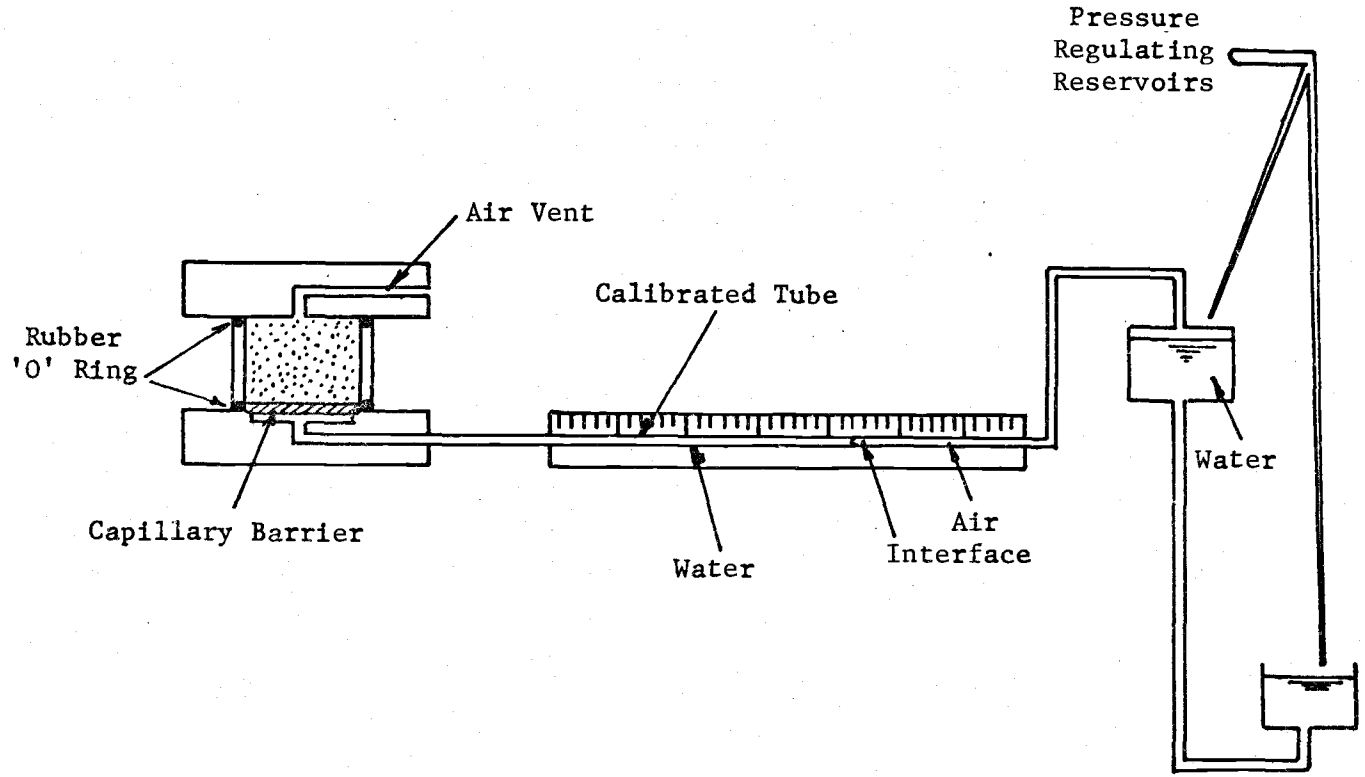

Figure 10. Apparatus for measuring capillary pressure head as a function of saturation on the soil cores.

close to saturation. At this time, it was connected to the U-tube and pressure regulating reservoirs. The capillary pressure was gradually increased in increments. At each value of pressure, the system was allowed to come to equilibrium and the position of the air-water interface noted in the U-tube. The pressure was increased to a maximum of 240 cm, then brought back down using the same procedure. In this way drainage and imbibition curves were obtained. After the runs, the U-tube distances were converted to volumes and then to saturations after the samples had been weighed and vacuum saturated.

The big disadvantage to the procedure was that it required about one month to run each sample. Evaporation was a problem which was solved by placing the sample container into a sealed plastic bag.

Surface samples from each plot were taken a year later and run with a new technique which is presently being developed at Oregon State University. This technique requires only two days to obtain both the drainage and imbibition curves. This will be the subject of a later paper.

IV. RESULTS AND DISCUSSION

The infiltration capacity curve and the advance of the wetting front in the soil profile during infiltration reflects the total hydraulic behavior of the profile under infiltration. This hydraulic behavior is largely controlled by the hydraulic properties of the soil matrix. Since the hydraulic properties of soils as defined by Brooks and Corey (1964) are determined primarily from capillary pressure-saturation curves, the major experimental effort was to obtain these curves *in situ* during infiltration. Hopefully the effect of these hydraulic properties upon the infiltration capacity curve and the advance of the wetting front could be observed.

However, this thesis will make no attempt to correlate the hydraulic properties of the soil with the hydraulic behavior during infiltration except in a limited qualitative manner. A quantitative correlation can best be accomplished on a digital computer using a mathematical model such as the work reported by Jeppson (1970 and in press). The purpose of presenting this experimental data is to provide some field data that may serve as a reference for other infiltration work which may be useful to those working with mathematical or empirical models.

Infiltration tests were made on six plots at sites indicated in Figure 1. The soil description of these sites are given in the Appendix. The soil surface condition of each test plot is given in Table I. The surface description is characterized as vegetation, litter, rocks, and bare soil all expressed as a percentage of the total surface area.

TABLE I. SOIL SURFACE CONDITION OF INFILTRATION PLOTS.

Plot number	Vegetation %	Litter %	Rock		Bare ground %
			Large (1"+) %	Small (1/8-1") %	
68057396					
68057196	14.57	2.24	0.28	12.32	70.59
68098Y97	35.55	38.67	1.17	0.00	24.61
68098Z97	39.26	10.40	5.37	10.07	34.90
68127D07	53.55	8.66	3.54	20.08	14.17
68127F07	42.66	13.30	9.97	28.25	5.82

The data obtained during infiltration are presented graphically in Figures 11-16. Each figure is for a separate infiltration plot. The last three digits of the plot number will be used as a shorthand reference to the plots. Later in this chapter, capillary pressure-saturation data obtained from soil cores taken in the infiltration plots will be shown in Figures 17-21 for both imbibition and drainage. These data then will be compared with the *in situ* data obtained during infiltration shown in Figures 22-25.

Field Data During Infiltration

The capillary pressure-saturation data and advance of the wetting front were obtained *in situ* under rainfall rates of either 1.27 or 1.78 cm/hr , which was low enough to prevent runoff from occurring. The infiltration rate as a function of time or the infiltration capacity curve was obtained at rates from 5.1 to 7.6 cm/hr. The exact rate is indicated on the (f) part of each figure. The infiltration capacity

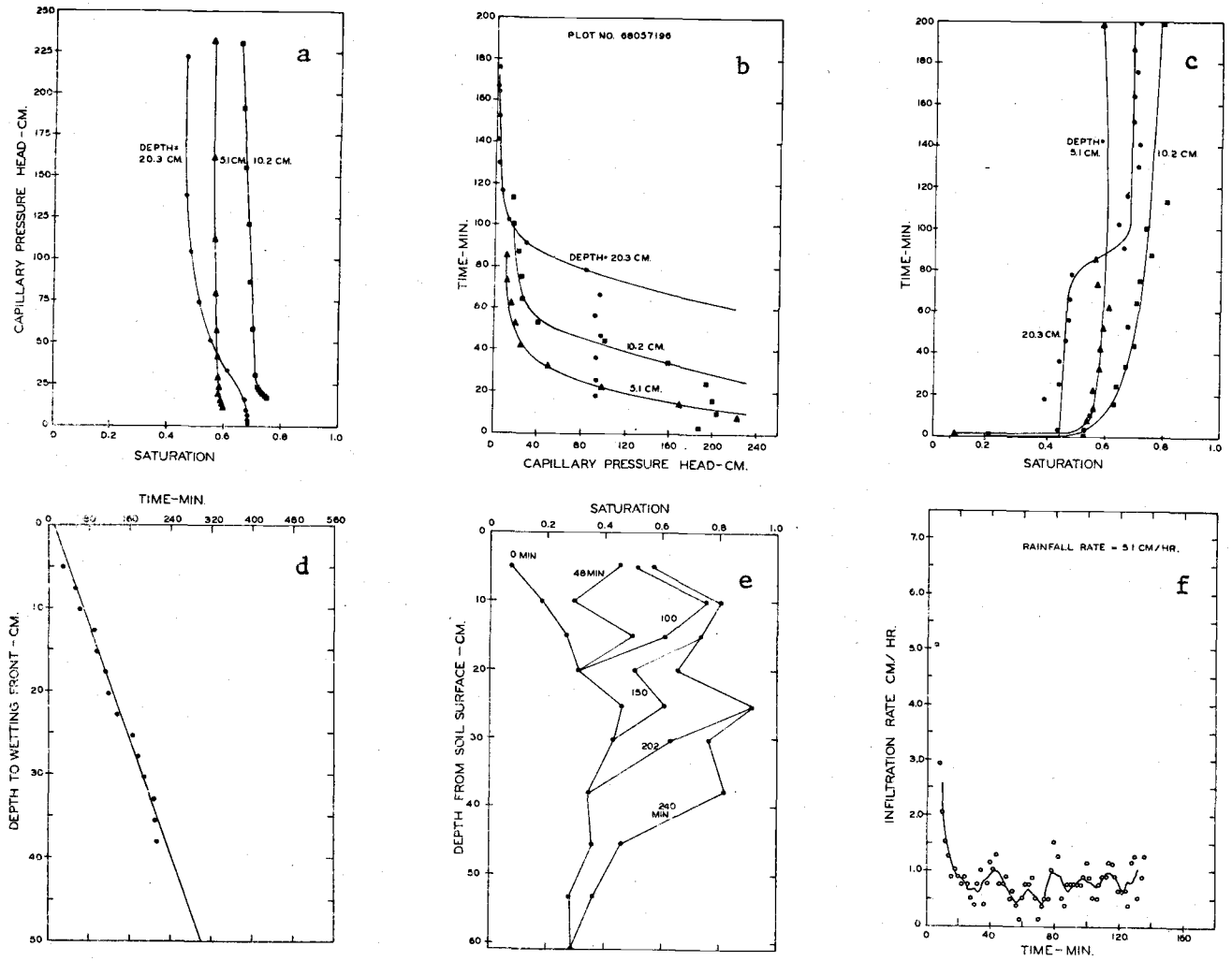

Figure 11. Capillary pressure head, saturation, wetting front, and infiltration rate as a function of time and profile depth for plot 196.

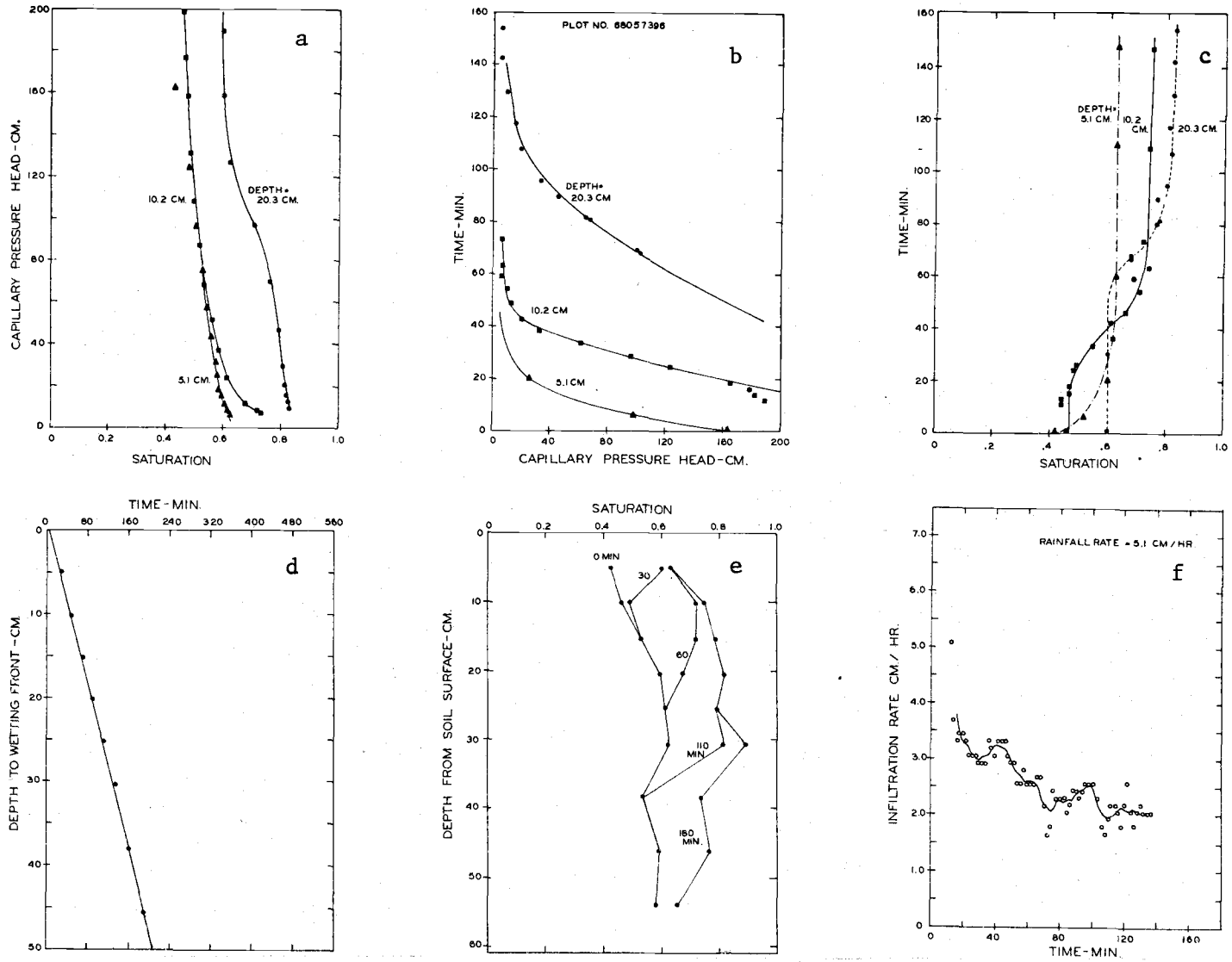

Figure 12. Capillary pressure head, saturation, wetting front and infiltration rate as a function of time and profile depth for plot 396.

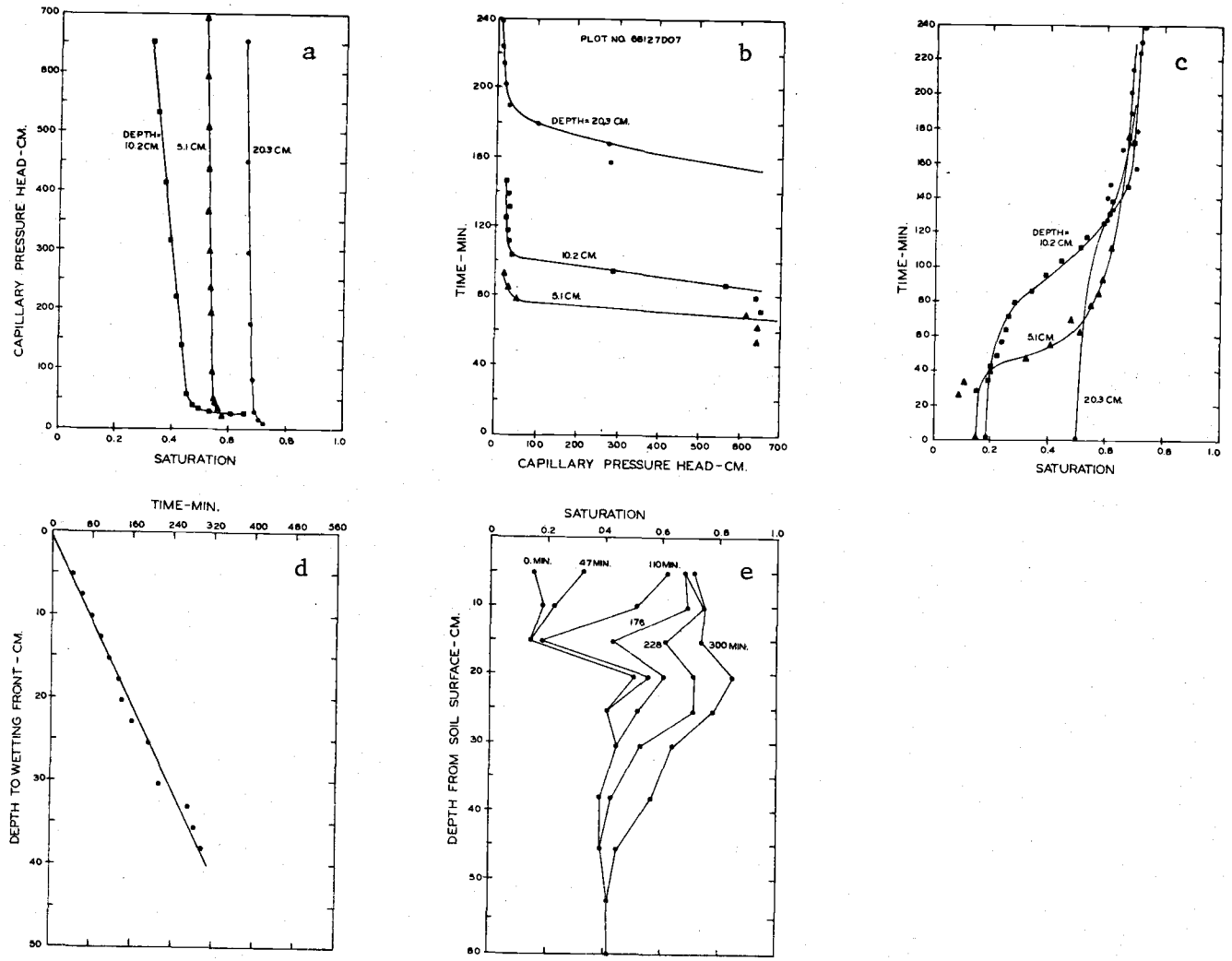

Figure 13. Capillary pressure head, saturation, wetting front, and infiltration rate as a function of time and profile depth for plot D07.

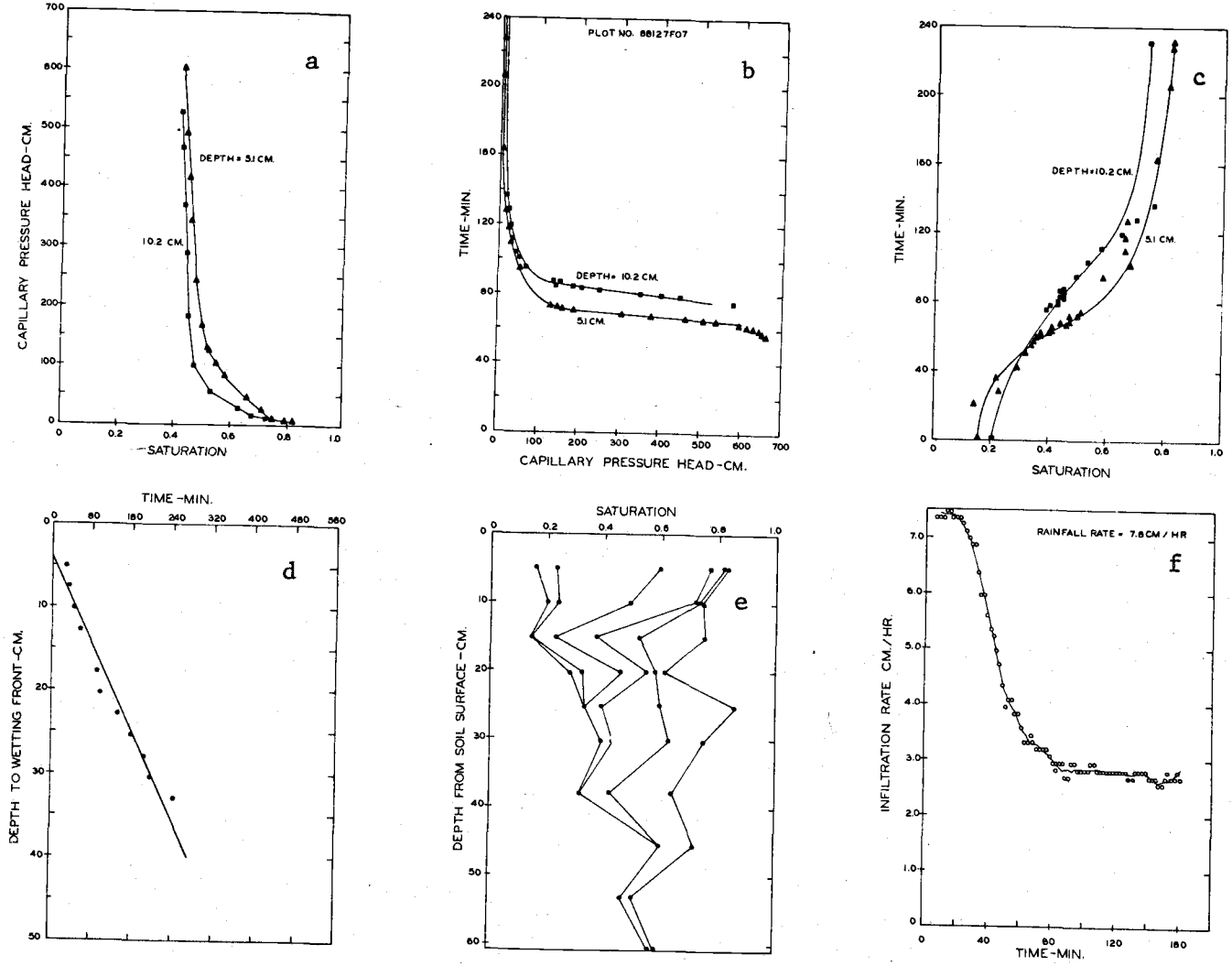

Figure 14. Capillary pressure head, saturation, wetting front, and infiltration rate as a function of time and profile depth for plot F07.

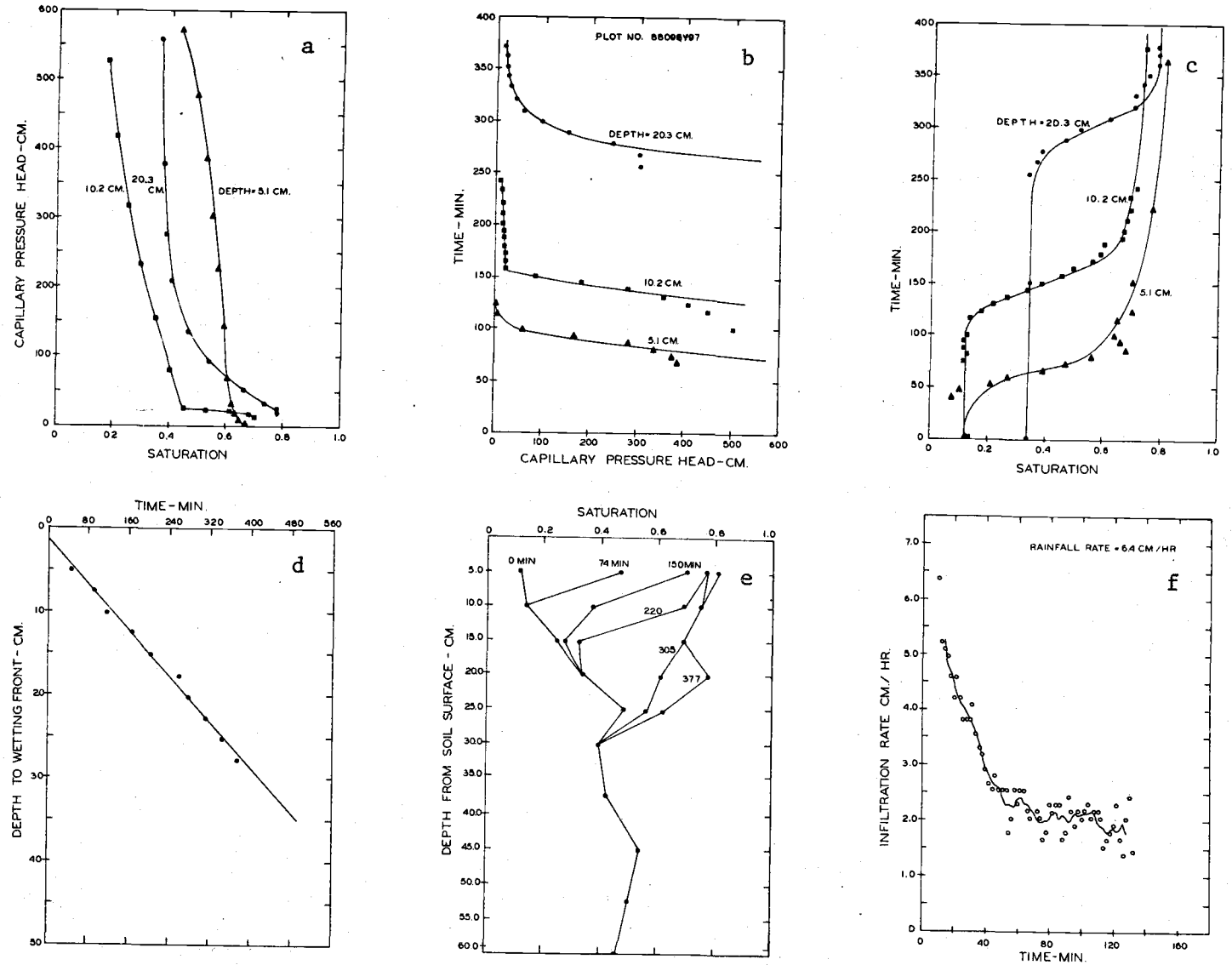

Figure 15. Capillary pressure head, saturation, wetting front and infiltration rate as a function of time and profile depth for plot Y97.

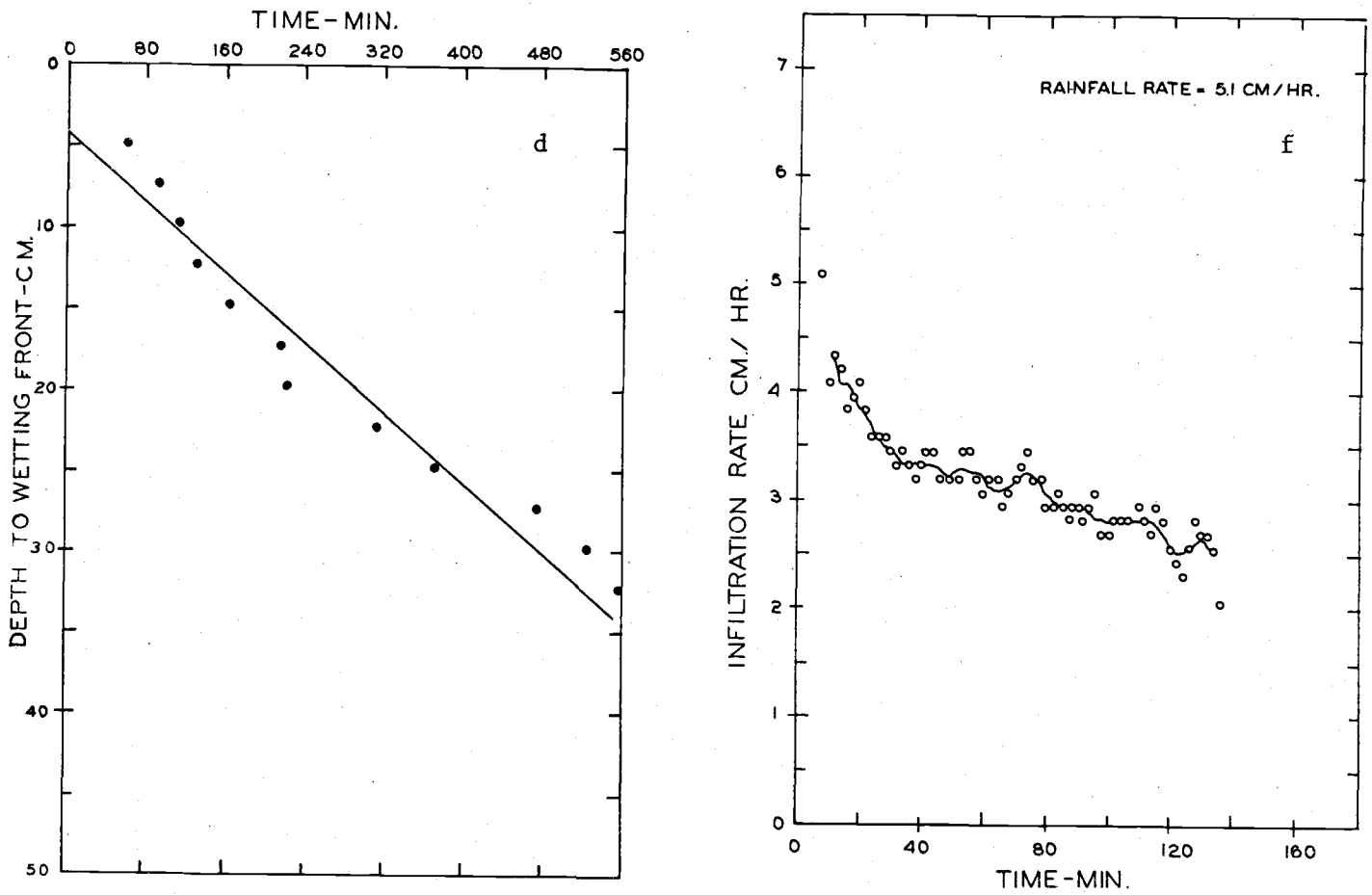

Figure 16. Wetting front and infiltration rate as a function of time for plot Z97.

curve was smoothed using a five point moving mean so that trends in the data could be seen more easily.

Since both capillary pressure and saturation had to be measured independently as a function of time and at different locations in the same profile, it was necessary to extrapolate and smooth the data so that capillary pressure could be correlated with saturation at selected times. The capillary pressure--time data were extrapolated because the tensiometers were installed before water was applied to the plots. The soil initially was quite dry and the capillary pressure of the soil was far beyond the limits of a tensiometer. In order to keep the tensiometers on scale and prevent air from entering the unit, a small amount of water was allowed to imbibe into the soil through the tensiometer. Therefore, the actual capillary pressures were much higher than those measured at the time the wetting front arrived. Thus, a smooth curve was drawn through the data points and extrapolated to values of capillary pressure higher than those measured when the wetting front arrived. The saturation data as a function of time were smoothed by drawing smooth curves which were best fitted by eye through the data points.

The capillary pressure head as a function of saturation was constructed by plotting saturation and capillary pressure head at selected times. The points shown in the (a) part of Figures 11-16 are not experimental but are those points that were obtained from the capillary pressure and saturation time curves at arbitrarily selected times.

Figures 11 and 12 show the data for Plots 196 and 396. These profiles are described in the Appendix as Nannyton loam which is a

fine textured loamy soil. From this profile description there appears to be a B-Horizon that should impede downward flow of water. The data in Figure 11(e) where saturation is plotted as a function of depth and time show that the saturation increases slightly with depth and then decreases to near the initial moisture content. This hydraulic behavior indicates that a restrictive layer may exist at a depth of 20 to 30 cm which is verified by the physical description.

The advance of the wetting front is shown to be a linear function of time in Figures 11(d) and 12(d). The relatively steep slope of these two curves indicate that the two profiles are relatively permeable. In Figures 11(d) and 12(d) the depth to wetting front as a function of time remains linear over a depth of almost 50 cm. In some previous work by King (1964) on one dimensional vertical imbibition in completely homogeneous profiles, the depth to the wetting front after a short period of time was shown to be linearly related to time. Therefore, the relationship of depth to the wetting front as a function of time for these infiltration plots is relatively insensitive to the layering noted in the profile description in the Appendix.

An examination of the *in situ* capillary pressure-saturation curves in Figures 11(a) and 12(a) for this Nannyton profile reveals an apparent variability that seems to exist in the hydraulic properties of the layers, i.e., the capillary pressure-saturation curves are not the same for each layer. However, if one knew how to take into account the variable volume of air entrapped at capillary pressures near zero, the capillary pressure-saturation curves for each depth may reduce to the same curve by using the similarity criteria proposed by Brooks and

Corey (1964). For instance, the shapes of the 20 cm depth curves are somewhat geometrically similar as are the curves for the 5 and 10 cm depth. The fact that the infiltration rate curves are different in Figure 11(f) and 12(f) during early stages of infiltration largely may be due to the difference in initial water contents of the upper layers of the profile and not due to differences in hydraulic properties of the two profiles.

The data shown in Figures 13 and 14 are for a Searla gravelly loam soil. This material has a significant quantity of large and small stones in the profile. In Figure 13 there appears to be a layer of finer texture at about 20 cm. This is apparent in the capillary pressure-saturation curve where the 20 cm depth holds much more water than those depths at 5 and 10 cm. Likewise, the initial saturation as a function of depth shows that the saturation at 20 cm is about 50 percent while that in the surface layers is about 18 percent. In spite of this, the depth to wetting front as a function of time remains linear over a depth of 40 cm.

The data shown in Figure 14 indicates the profile is more uniform in its properties and hydraulic behavior.

Saturation as a function of depth and time in Figure 14(e) increases in a manner that is similar to homogeneous profiles. The capillary pressure-saturation curve at the 5 and 10 cm depth is practically the same. Data in Figure 14(f) for infiltration capacity curve is much smoother than for any other run. However, the advance of the wetting front with time appears slightly curvilinear in spite of the fact that a straight line was drawn to approximate the data points.

The data shown in Figures 15 and 16 is for the Babbington loam, a fine loamy soil. According to the soil classification description in the Appendix, a B-Horizon exists a few centimeters below the soil surface. The presence of this less permeable layer is primarily noted in the capillary pressure-saturation data where the 5 cm depth holds substantially more water than the deeper layers. The rate of advance of the wetting front is much lower for Figures 15(d) and 16(d) than those previously shown. Satisfactory capillary pressure-saturation data was not obtained for Plot Z97. In Figure 16, only depth to the wetting front as a function of time and the infiltration capacity curve are shown for this profile.

Capillary pressure-saturation data obtained *in situ* for the profiles shown in Figures 11-15 were very difficult and tedious to obtain. In as much as the capillary pressure data was taken at a different depth in the profile, there was a very good possibility that the wetting front as measured by the gamma probe would not always reach the tensiometer at the same time indicated by the gamma probe. In fact, in most of the installations, the gamma probe indicated the wetting front several minutes before the tensiometer indicated the same wetting front. No attempt was made to correct for this lag of time in the capillary pressure data.

The capillary pressure-saturation data appeared to be very sensitive to the texture and layering that existed within the soil profile. It is difficult to see from the data presented here how the hydraulic properties of the soil as measured by the capillary pressure-saturation curves affect the infiltration process. In fact, unless the capillary

pressure-saturation data are scaled according to some similitude requirement, it will be impossible to determine whether or not the profiles are hydraulically similar.

Laboratory Data From Soil Cores

In order to determine the hydraulic properties for these soil profiles where infiltration measurements were made, "undisturbed" soil cores were taken at depths equal to the installation depths of the tensiometers. Capillary pressure-saturation data for both imbibition and drainage was obtained from these cores so that the hydraulic properties defined by Brooks and Corey (1964) could be determined under controlled laboratory conditions.

Laboratory data from these soil cores are shown in Figures 17-21. The data has been scaled and presented as relative capillary pressure as a function of effective saturation. Open squares represent data points for the drainage cycle while closed circles represent data points for imbibition cycle. The curves are drawn from the two equations

$$S_e = (P_c)^{-\lambda} \quad \text{, for drainage}$$

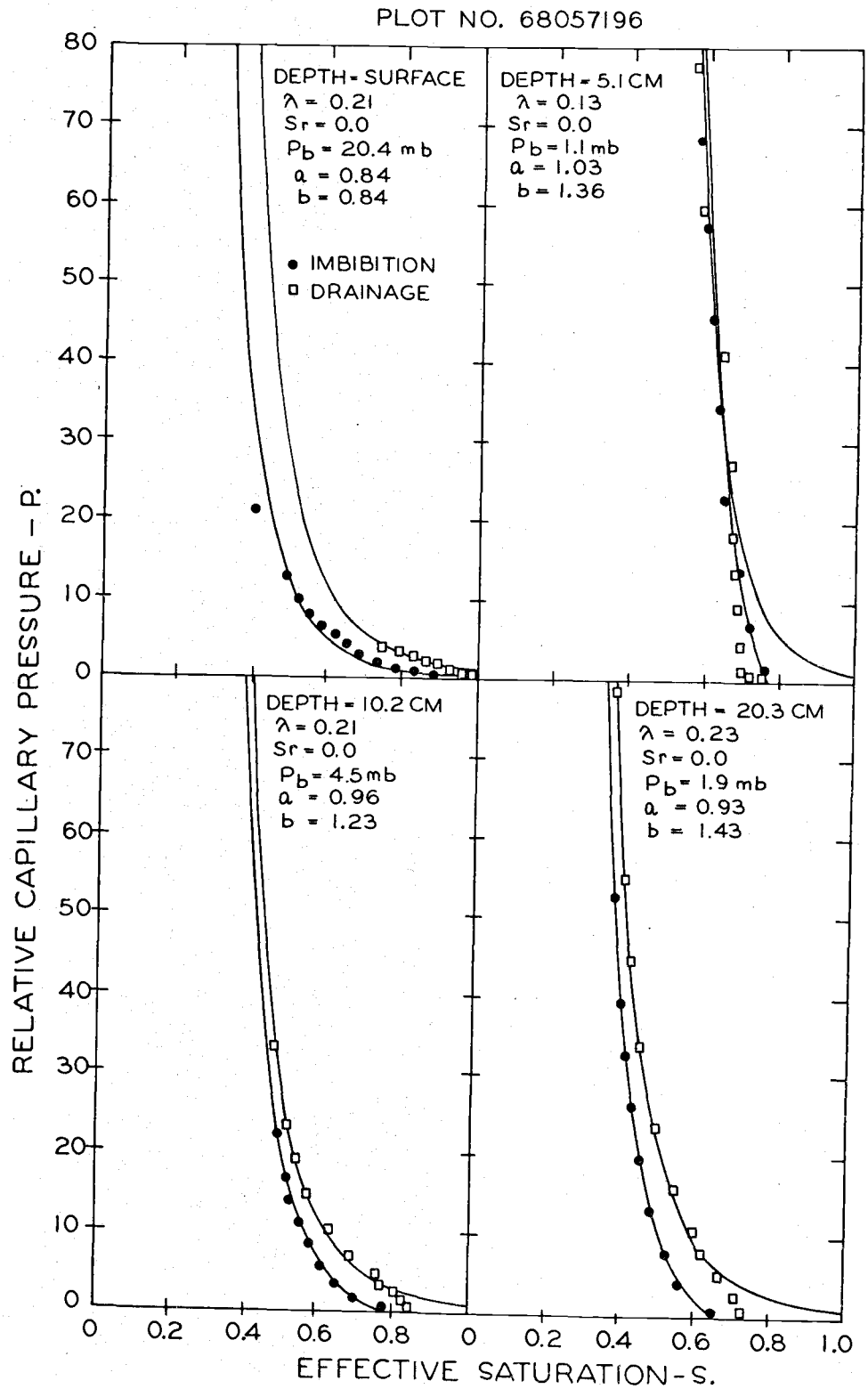

Figure 17. Experimental data for plot 196 and theoretical curves showing relative capillary pressure as a function of effective saturation obtained from soil cores for imbibition and drainage.

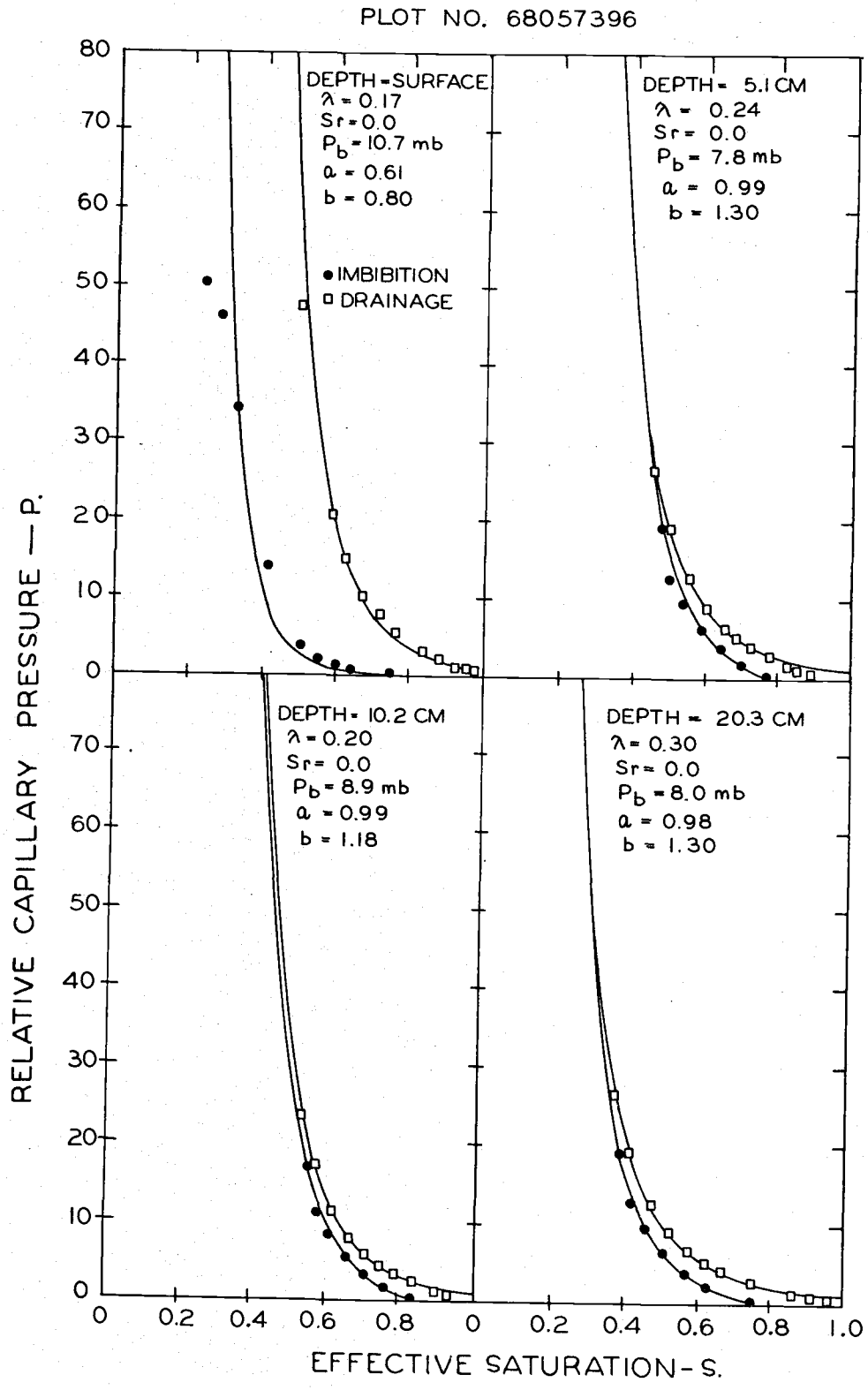

Figure 18. Experimental data for plot 396 and theoretical curves showing relative capillary pressure as a function of effective saturation obtained from soil cores for imbibition and drainage.

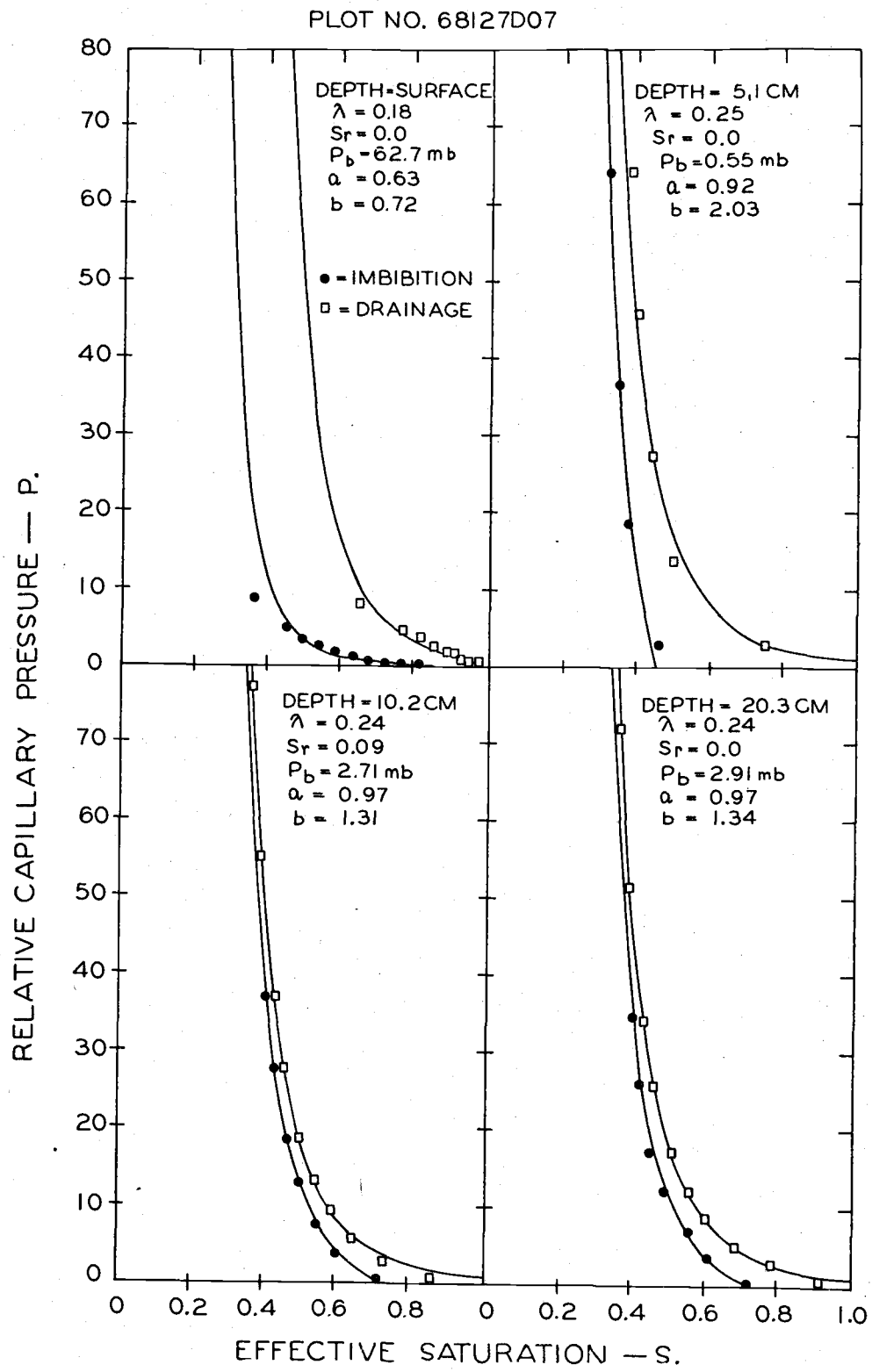

Figure 19. Experimental data for plot D07 and theoretical curves showing relative capillary pressure as a function of effective saturation obtained from soil cores for imbibition and drainage.

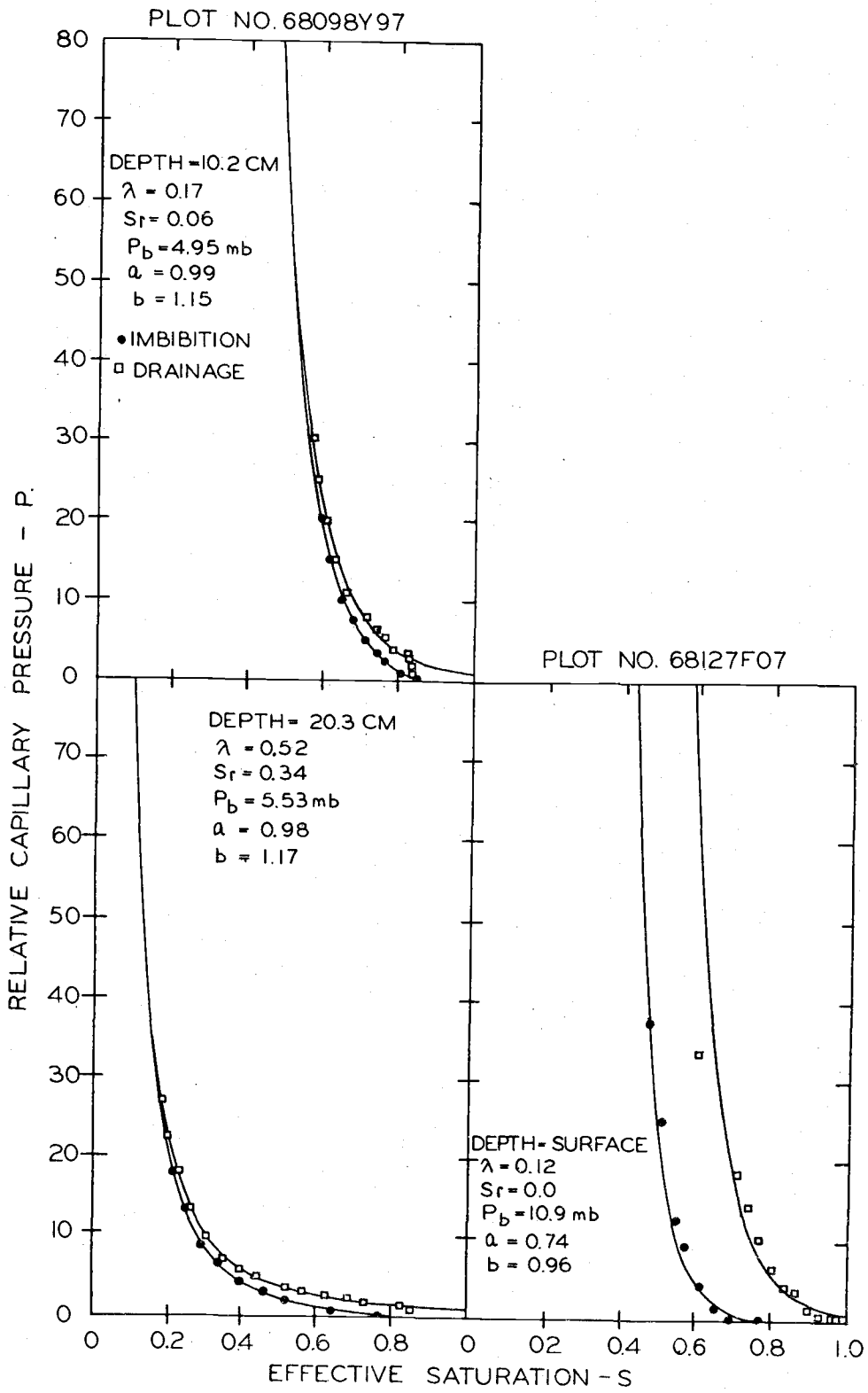

Figure 20. Experimental data for plots Y97 and F07 and theoretical curves showing relative capillary pressure as a function of effective saturation obtained from soil cores for imbibition and drainage.

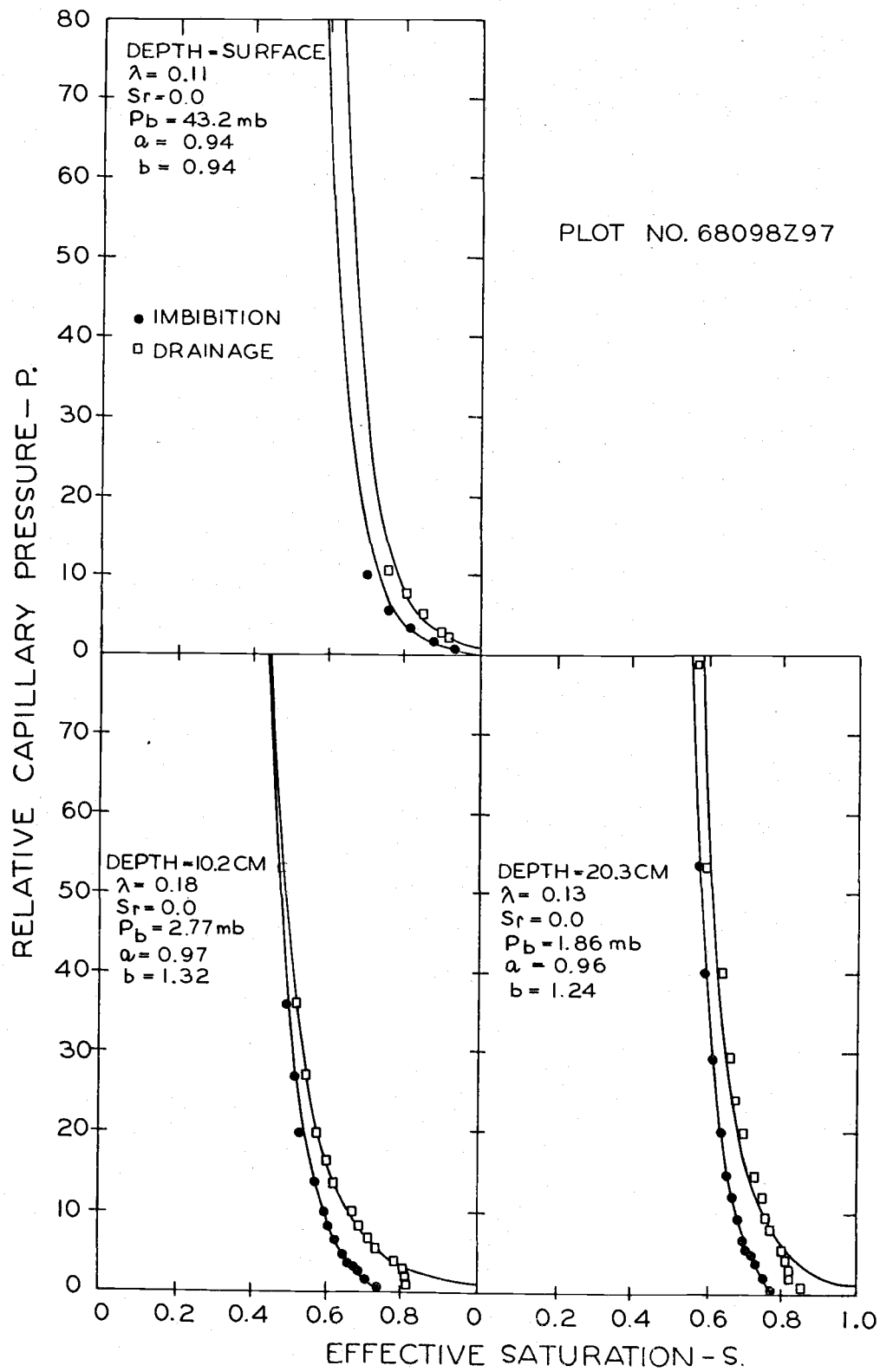

Figure 21. Experimental data for plot Z97 and theoretical curves showing relative capillary pressure as a function of effective saturation obtained from soil cores for imbibition and drainage.

and

$$S. = \frac{a}{(b^{1/\lambda} + P.)^{\lambda}}, \text{ for imbibition,}$$

where $S. = (S - S_r)/(1 - S_r)$ and $P. = P_c/P_b$. The parameter λ was defined by Brooks and Corey (1964) as the pore size distribution index and is determined only from the drainage capillary pressure-saturation curve as are the residual saturation, S_r, and the bubbling pressure, P_b. The constants a and b are dimensionless parameters that were chosen to give the best fit to the imbibition data. The parameters a, b, and λ are tabulated in Table II for each profile and for the various depths within the profile. If two soil samples are similar from a hydrodynamic point of view, then the parameters a, b, and λ must be identical for both. As noted from Table II, no two profiles upon which infiltration data were obtained are hydraulically similar, i.e., no two sets of samples have identical values of a, b, and λ.

It should be noted, however, that the values within a given profile are not greatly different. It is not known at this time how sensitive the hydraulic behavior of a profile is to these parameters. It is possible that for watershed management and runoff studies, average values for profiles may be acceptable in making predictions by the use of mathematical models.

Comparison of Field and Laboratory Data

Capillary pressure head and saturation as obtained from soil cores from various depths within the infiltration plots are compared with capillary pressure head and saturation data obtained under the

TABLE II. HYDRAULIC PROPERTIES OF SOIL CORES OBTAINED FROM INFILTRATION PLOTS.

Plot	Depth(cm)	λ	a	b	S_r	$P_b/\rho g$(Cm H_2O)
196	surface	0.207	0.84	0.84	0.00	20.85
	5.1	0.130	1.02	1.36	0.00	1.11
	10.2	0.210	0.96	1.23	0.00	4.60
	20.3	0.226	0.93	1.43	0.00	1.94
396	surface	0.169	0.61	0.80	0.00	10.90
	5.1	0.235	1.00	1.30	0.00	8.00
	10.2	0.199	0.99	1.18	0.00	9.09
	20.3	0.300	0.98	1.30	0.00	8.15
D07	surface	0.182	0.63	0.72	0.00	64.00
	5.1	0.247	0.93	2.03	0.00	0.56
	10.2	0.236	0.97	1.31	0.09	2.77
	20.3	0.240	0.96	1.34	0.00	2.97
F07	surface	0.121	0.75	0.96	0.00	11.14
	5.1	No Data				
	10.2	No Data				
	20.3	No Data				
Y97	surface	No Data				
	5.1	No Data				
	10.2	0.166	0.99	1.15	0.06	5.05
	20.3	0.518	0.98	1.17	0.34	5.64
Z97	surface	0.105	0.94	0.94	0.00	44.06
	5.1	No Data				
	10.2	0.181	0.98	1.32	0.00	2.83
	20.3	0.125	0.95	1.24	0.00	1.90

rainfall simulator. The curves drawn in Figures 22-25 were obtained from the data shown in the (a) parts of Figures 11-15 where capillary pressure was plotted as a function of saturation. The open circle points are data taken from Figures 17-21 for the imbibition cycle only where capillary pressure was plotted as a function of saturation. For some infiltration plots and for some depths the comparison between the field data and the laboratory cores is favorable. The most consistent

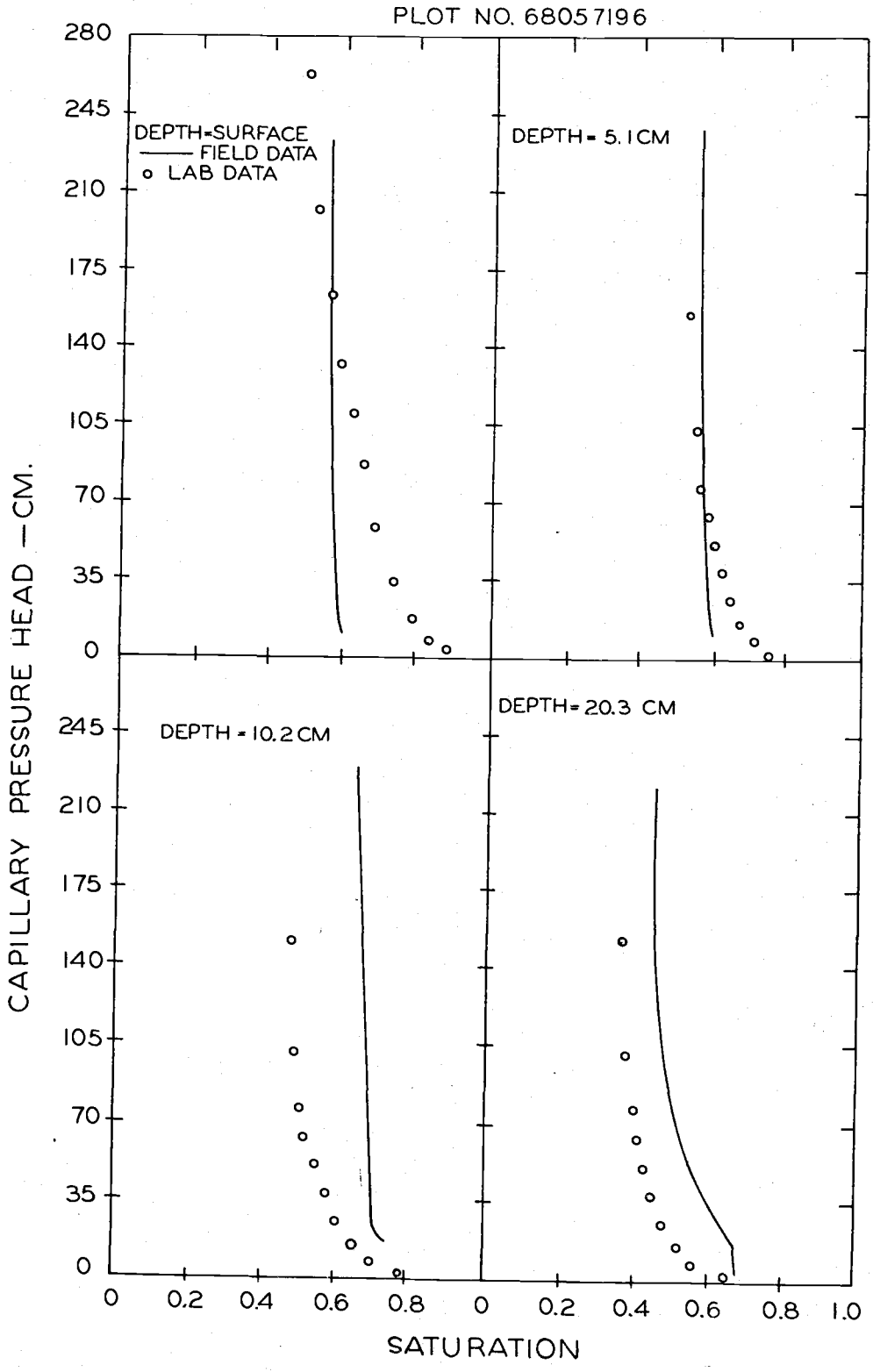

Figure 22. Capillary pressure as a function of saturation for *in situ* measurements in infiltration plot 196 and laboratory measurements on soil cores.

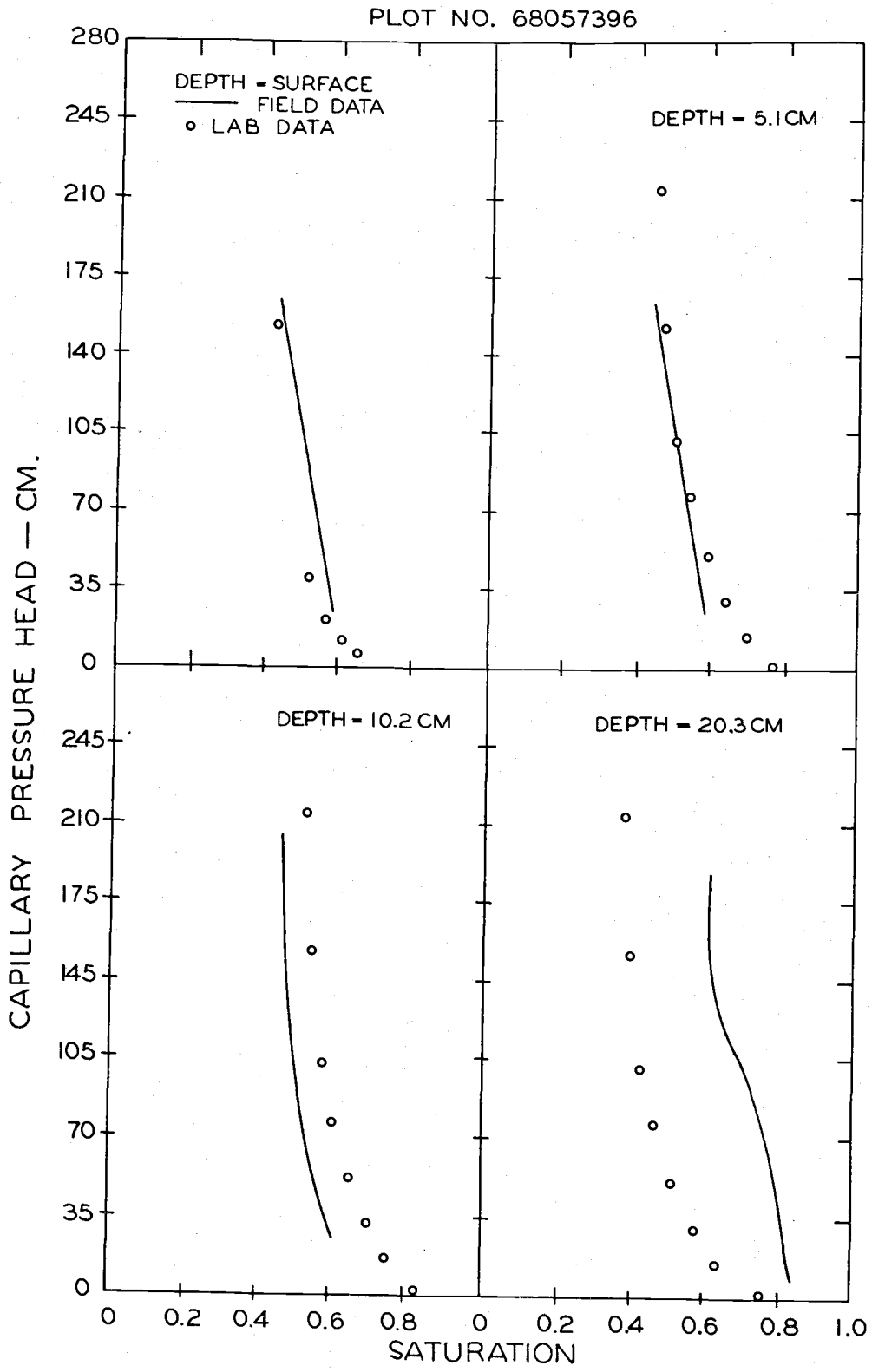

Figure 23. Capillary pressure as a function of saturation for *in situ* measurements in infiltration plot 396 and laboratory measurements on soil cores.

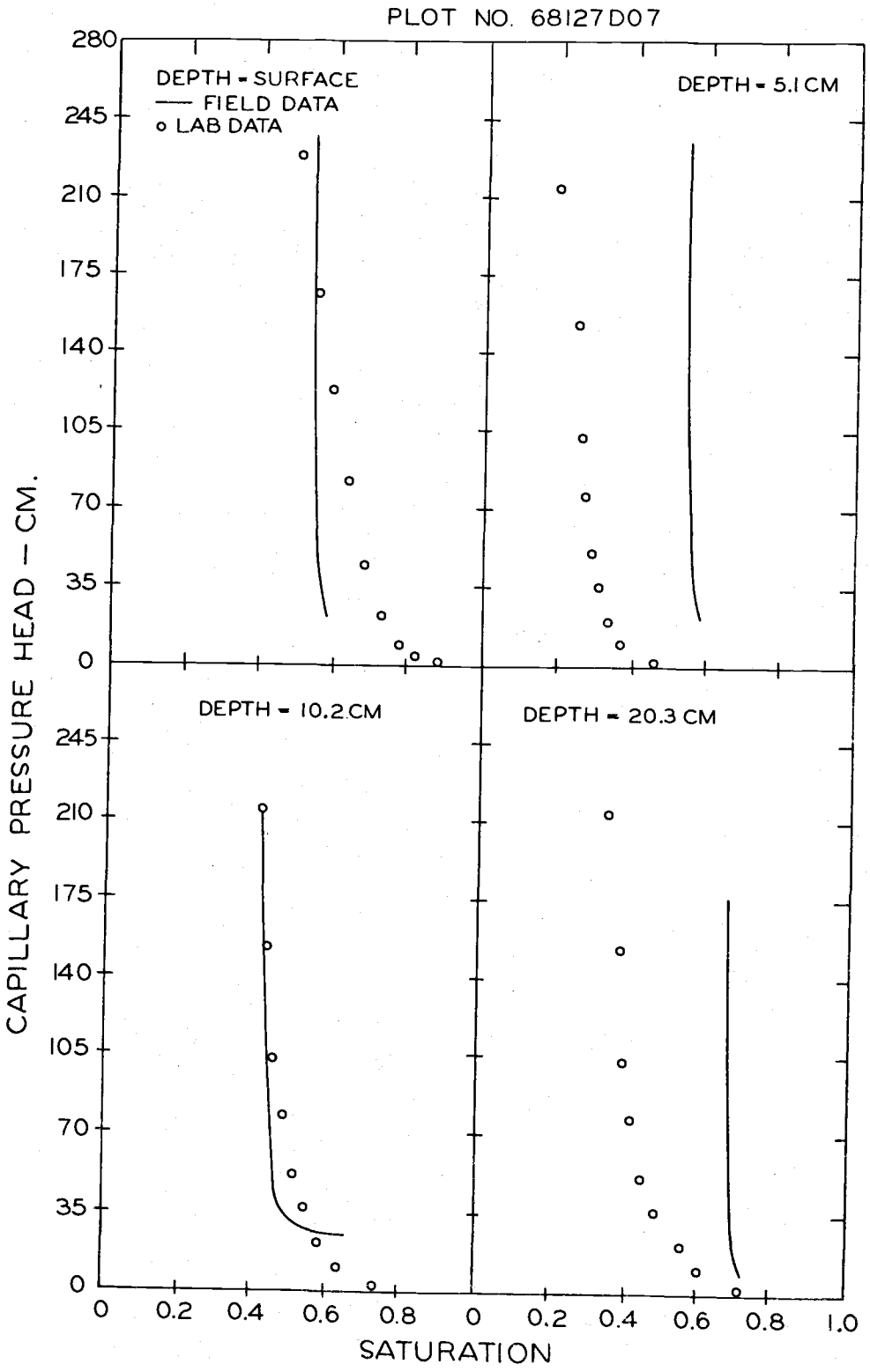

Figure 24. Capillary pressure as a function of saturation for *in situ* measurements in infiltration plot D07 and laboratory measurements on soil cores.

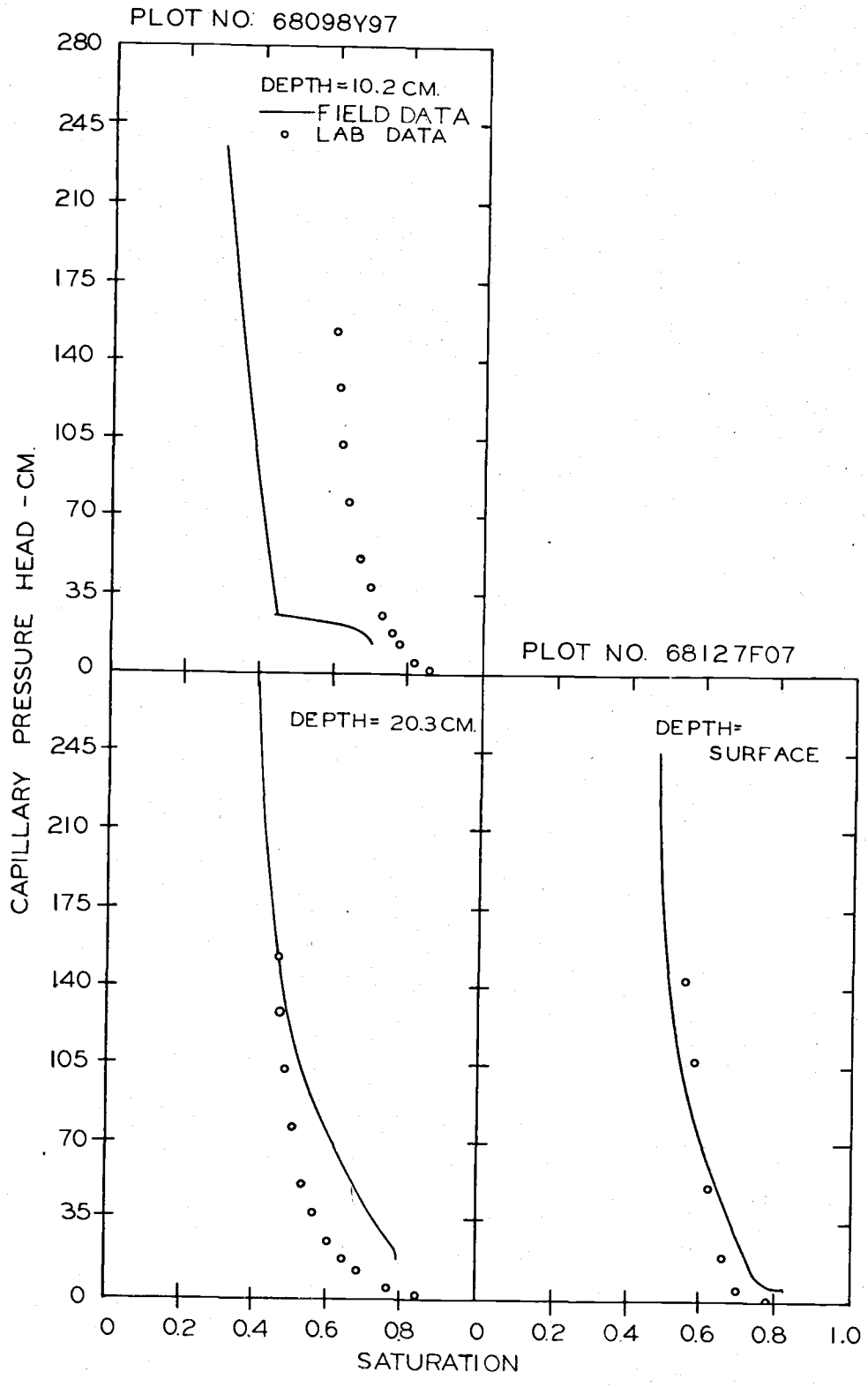

Figure 25. Capillary pressure as a function of saturation for *in situ* measurements in infiltration plots Y97 and F07 and laboratory measurements on soil cores.

and favorable comparisons are for those cores taken at the soil surface and at five cm below the soil surface.

It is quite likely that data obtained on soil samples taken from the field plots would not be the same as those measured *in situ*. This may be due in part to compaction of the soil sample during its removal from the profile and the subsequent disturbance in the laboratory due to wetting and drying of the sample. It is well known that soil cores removed from the field to the laboratory for purposes of measuring the saturated hydraulic conductivity seldom agree with those measurements taken in the field. Therefore, these differences between laboratory cores and field measurements of capillary pressure and saturation are not particularly surprising and are probably as good a comparison as one could expect.

In Figure 26 the infiltration capacity curves for all the field infiltration plots are replotted in terms of scaled variables. The standard unit of infiltration rate is the saturated hydraulic conductivity and the standard unit of time defined by Brooks and Corey (1964) is

$$t_* = \frac{(\rho g)^2 k}{\mu P_b \phi_e} t = \frac{K}{P_b/(\rho g)\phi_e} t \quad .$$

The saturated hydraulic conductivities used to scale the infiltration rates were determined by using the apparent asymptotic infiltration rate from data shown in the (f) part of Figures 11-16. The scaling factors that were used are given in Table III. All of the curves in Figure 26, therefore, approach a scaled infiltration rate equal to unity. By using scaled variables it is now permissible to compare

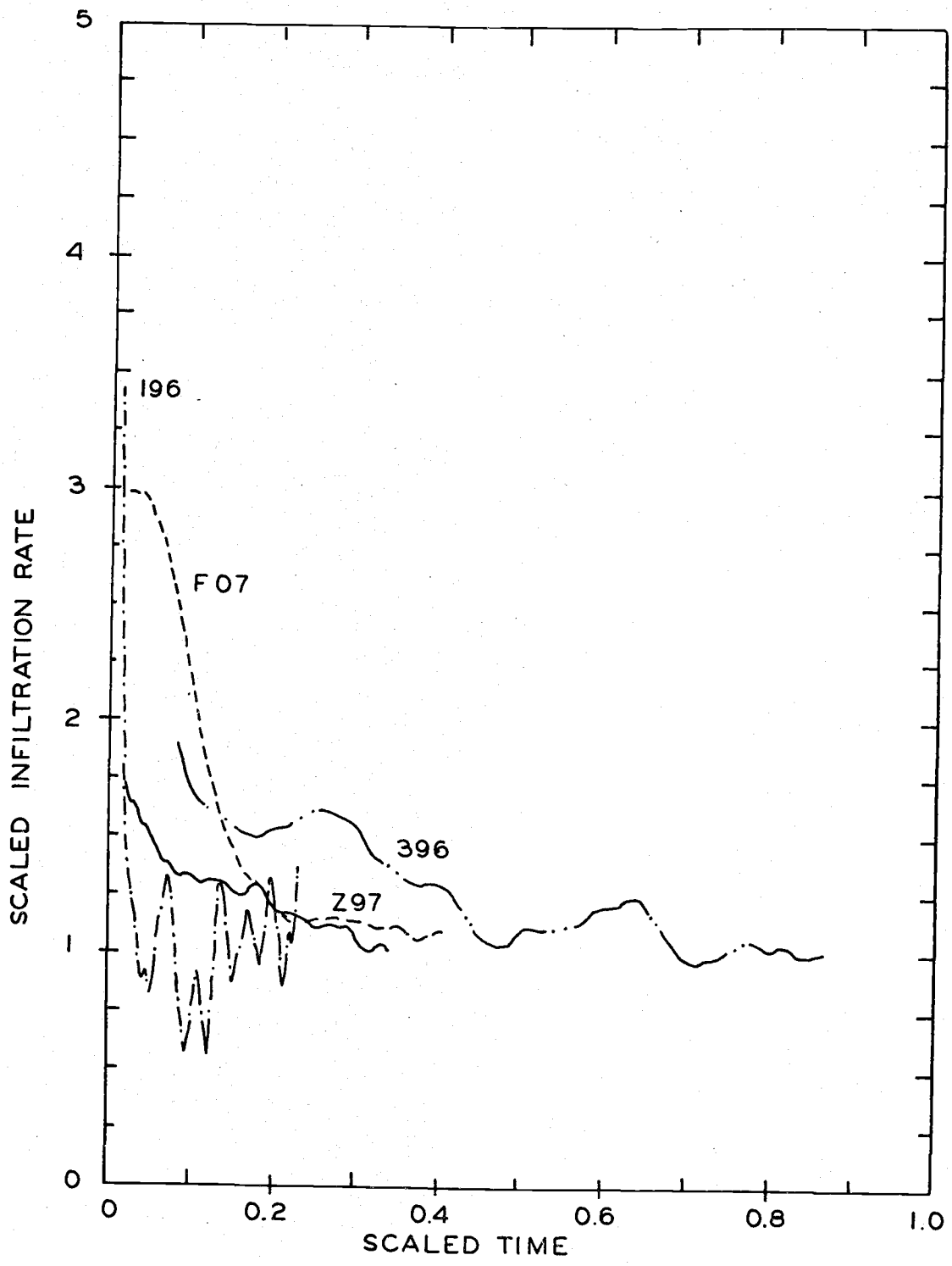

Figure 26. Comparison of the scaled infiltration rate as a function of scaled time for four infiltration plots.

TABLE III. SCALING FACTORS FOR THE INFILTRATION RATE AS A FUNCTION OF TIME DATA OBTAINED FROM THE INFILTRATION PLOTS.

Plot	K(cm/hr)	$P_b/\rho g$ (Cm H_2O)	ϕ_e
196	0.75	21	0.33
396	2.00	11	0.45
Z97	2.50	44	0.36
F07	2.75	11	0.54

the infiltration capacity curves for each of the four plots. It is interesting to observe again that for Plots 196 and 396 where the soil classification is apparently the same, the infiltration capacity curves are vastly different. Of course, some of these differences may in fact be due largely to initial conditions and the difference in surface conditions of the plot, e.g., the percent of vegetative cover on the plot. For the four plots shown, Plot F07 has the highest percentage of vegetation and the lowest percentage of bare soil, 43 and 6 percent respectively. On the other hand, for Plot 196, vegetative cover was only 14.6 percent with the bare soil being 71 percent. The infiltration rate for Plot 196 drops off abruptly as a function of scaled time. Runoff will, therefore, occur more readily from the portion of the watershed represented by Plot 196 and is less likely to occur on plots like F07 where the vegetative cover is relatively high. These facts are not new, as it is well known that on soils where vegetative cover is present the infiltration will always be higher than on bare soils where there is an absence of vegetative cover. The use of

scaled infiltration rate and scaled time, however, allows one to compare various soil textures as well as various surface conditions.

V. SUMMARY AND CONCLUSIONS

A rainfall simulator was used to study infiltration on six soil profiles on the Reynolds Creek Watershed in the semi-arid region of Southwestern Idaho. Capillary pressure and soil-water content was measured during infiltration at rates that would not cause runoff. The infiltration sites were typical of many semi-arid soil profiles having varying degrees of subsurface layering and vegetative cover. Infiltration capacity curves were obtained on the sites with rainfall rates of five to seven cm/hr. Soil cores were removed from the infiltration sites at the conclusion of each test and taken to the laboratory where capillary pressure-saturation relationships were determined for both imbibition and drainage cycles. These data were compared with *in situ* measurements obtained during infiltration.

Large rainfall simulators such as the one described in this report that cause rainfall to occur over a square area 1.83 m by 1.83 m produce infiltration that is essentially one-dimensional in character. A gamma-ray probe and three tensiometers were used to measure capillary pressure and saturation during infiltration at low precipitation rates. The tensiometers and gamma-ray probes were located approximately near the center of the infiltrating area but at different locations. If the profile is assumed to be homogeneous with respect to any given depth and the flow is assumed to be one-dimensional, then one should be able to correlate capillary pressure with saturation even though the measurements are taken at different locations. These relationships were determined and presented in Chapter

IV. Because these assumptions were not proven, the *in situ* capillary pressure-saturation data may not truly be representative of the depth indicated.

The similarity of the *in situ* capillary pressure-saturation data from one depth to another actually may be better or worse than what was shown. It therefore does not seem practical to use the techniques described herein for obtaining *in situ* capillary pressure saturation data. The measurements taken in the field are still point measurements in the profile and it will probably be easier and more economical to remove these profile points for measurement in the laboratory. The problem with removal to the laboratory is disturbance.

It is conceivable to use capillary pressure-saturation data to predict infiltration and runoff but it may not be economical or practical. One may eventually conclude that soil can be broadly classified according to some profile pore size distribution index that can be used to make sufficiently accurate predictions using mathematical models. An imbibition profile property such as an average pore size distribution index perhaps can be correlated with some simple field technique that integrates many factors into a single profile characteristic.

Based upon the results presented herein, it appears that the surface layers of the profile have a predominant effect upon the hydraulic behavior of the entire profile under infiltration. The classification of the surface layers according to their hydraulic characteristic may be the only part of the profile that needs to be considered for predicting infiltration.

In conclusion, to predict infiltration or runoff from ungauged profiles or watersheds continues to be an extremely difficult task. Hopefully these field and laboratory data will lead others to the development of predictive models that can be used with on-site measurements.

Finally, these data may be used by those working with mathematical models for purposes of verifying a model that requires capillary pressure-saturation data.

VI. FUTURE RESEARCH

If future tests are conducted with the field equipment used in this study, the following improvements should be made:

1. Tensiometers should be used which have the capillary barrier on the side instead of on the bottom. This would allow the wetting front to be sensed when it actually arrives at the level of the capillary barrier instead of having to wait for horizontal moisture movement to reach it.
2. Use tensiometers which are mounted on the same probe. This would reduce the error in the depth at which they are installed.
3. Insulate the nylon tubing which connects the tensiometers to the pressure transducers. This would reduce variations in the capillary pressure data which is due to temperature changes.
4. Obtain gamma density data only where the gamma counts are changing significantly with time. This would give more saturation data to be correlated with capillary pressure data when the wetting front reaches the depth of each tensiometer.

BIBLIOGRAPHY

1. Brooks, R. H. and A. T. Corey. Hydraulic properties of porous media. Hydrology Paper No. 3, Colorado State University, Fort Collins, Colorado. 1964.

2. Burgy, R. H. and J. N. Luthin. A test of the single and double ring types of infiltrometers. Transactions of the American Geophysical Union, 37:189-191. 1956.

3. Colman, E. A. and G. B. Bodman. Moisture and energy conditions during downward entry of water into moist and layered soils. Soil Science Society of America Proceedings 9:3-11. 1945.

4. Hanks, R. J. and S. A. Bowers. Numerical solution of the moisture flow equation for infiltration into layered soils. Soil Science Society of America Proceedings, 26:530-534. 1962.

5. Jeppson, R. W. Determination of hydraulic conductivity-capillary pressure relationship from saturation-capillary pressure data from soils. PRWG-59c-4, Utah Water Research Laboratory, Utah State University, Logan, Utah. July 1970.

6. Jeppson, R. W. Solution to transient vertical moisture movement based upon saturation-capillary pressure data and a modified Burdine Theory. PRWG-59c-5, Utah Water Research Laboratory, Utah State University, Logan, Utah. December 1970.

7. Jeppson, R. W. Solutions to axisymmetric infiltration. Journal of the Hydraulics Division, American Society of Agricultural Engineers. (In press.)

8. King, L. G. Imbibition of fluids by porous solids. A Ph.D. dissertation submitted to Colorado State University, Fort Collins, Colorado. December 1964.

9. Miller, D. E. and Wm. C. Bunger. Moisture retension by soil with coarse layers in the profile. Soil Science Society of America Proceedings 27:586-589. 1963.

10. Penton, V. E. and W. R. Hamon. A rainfall simulator, gamma probe infiltrometer. (In press.)

11. Robins, J. S., L. L. Kelly, and W. R. Hamon. Reynolds Creek in southwest Idaho: an outdoor hydrologic laboratory. Water Resources Research 1:407-413. 1965.

12. Shull, H. Influence of installation depth on infiltration from unbuffered cylinder infiltrometers. Soil Science 97:279-280. 1964.

13. U.S. Soil Survey Staff. Soil Survey Manual, U.S. Department of Agriculture Handbook No. 18:503. 1962.

14. Wilm, H. G. Methods for the measurement of infiltration. Transactions of the American Geophysical Union 22:678-686. 1941.

15. Wisler, C. O. and E. F. Brater. Hydrology. John Wiley and Sons Inc. New York. Second Edition. 1967.

APPENDIX A

Data from Field Plots and Laboratory Cores regarding capillary pressure, saturation, infiltration rate and wetting front advance.

TABLE A I. IMBIBITION SATURATION AND CAPILLARY PRESSURE HEAD DATA OBTAINED FROM INFILTRATION PLOTS.

5.1 cm depth			10.2 cm depth			20.3 cm depth		
Time (min.)	P_c(Cm H_2O)	Sat. (%)	Time (min.)	P_c(Cm H_2O)	Sat. (%)	Time (min.)	P_c(Cm H_2O)	Sat. (%)
Plot 68057196								
1	253	44	0	206	53	18	94	39
8	222	54	3	188	53	25	94	44
14	170	56	10	204	55	36	94	44
22	99	56	16	199	63	46	98	46
32	50	58	24	194	64	56	43	47
42	25	58	34	160	67	66	96	47
52	20	59	44	101	70	78	84	48
62	16	61	53	41	68	91	29	66
73	12	57	64	26	71	102	13	64
85	12	56	75	24	72	116	7	67
			87	22	76	130	4	71
			100	18	74	141	2	71
			113	17	81	152	4	69
						164	2	69
						176	4	70
						187	2	69
						202	3	71
Plot 68057396								
0	163	42	11	189	44	0	96	60
6	98	52	13	182	44	67	103	68
20	26	60	15	179	47	68	102	68
			18	165	47	80	69	77
			24	124	48	81	65	78
			28	96	49	89	47	79
			33	62	55	95	35	80
			38	33	62	107	21	82
			42	21	61	117	17	81
			48	14	66	129	11	82
			54	10	71	142	7	82
			59	7	69	154	7	83
			63	7	74			
			73	7	72			

TABLE A I. (CONTINUED).

5.1 cm depth			10.2 cm depth			20.3 cm depth		
Time (min.)	P_c(Cm H_2O)	Sat. (%)	Time (min.)	P_c(Cm H_2O)	Sat. (%)	Time (min.)	P_c(Cm H_2O)	Sat. (%)
Plot 68127D07								
54	643	41	71	652	26	157	280	70
62	645	51	79	642	28	168	275	65
69	616	48	86	566	34	179	100	70
77	53	55	94	288	39	189	27	68
84	32	57	103	41	44	201	17	68
92	23	59	111	34	51	214	14	69
			117	31	53	224	12	71
			125	27	59	240	11	73
			131	34	61	253	10	72
			138	31	62	266	7	77
			146	25	67			
Plot 68127F07								
56	663	34	75	582	39			
57	653	35	78	452	40			
59	646	36	79	405	43			
60	632	37	80	352	43			
61	615	37	82	252	45			
62	598	40	83	208	44			
64	539	41	84	188	45			
65	509	41	85	144	45			
66	464	46	86	157	44			
67	380	44	87	140	45			
68	307	47	95	68	49			
70	189	47	103	43	53			
71	161	47	111	33	58			
72	149	50	119	30	65			
73	131	51	128	26	70			
94	55	59	136	16	76			
101	50	68						
109	31	66						
117	25	66						
127	18	67						
163	7	77						
205	5	81						
227	3	82						

TABLE A I. (CONTINUED).

5.1 cm depth			10.2 cm depth			20.3 cm depth		
Time (min.)	P_c(Cm H_2O)	Sat. (%)	Time (min.)	P_c(Cm H_2O)	Sat. (%)	Time (min.)	P_c(Cm H_2O)	Sat. (%)
Plot 68098Y97								
66	386	39	100	504	12	255	303	33
72	373	47	116	449	15	267	301	36
79	336	56	123	407	19	277	246	38
85	283	68	130	357	21	288	154	46
92	169	66	137	280	26	298	98	51
98	60	64	144	183	34	308	58	61
114	6	66	150	86	38	320	40	70
122	3	70	157	24	45	331	29	70
			164	24	49	342	23	73
			171	23	56	351	21	75
			178	20	59	361	19	78
			187	19	60	370	16	78
			193	17	66			
			200	17	67			
			210	16	68			
			220	16	69			
			232	13	69			
			241	11	71			

TABLE A II. TIME AND DEPTH TO WETTING FRONT OBTAINED FROM INFILTRATION PLOTS.

Time from start of rain (minutes)	Depth from surface to wetting front (inches)
Plot 68057396	
30	2
50	4
72	6
90	8
114	10
138	12
162	15
190	18
Plot 68098Z97	
61	2
93	3
116	4
133	5
166	6
218	7
225	8
315	9
374	10
476	11
527	12
560	13
Plot 68127D07	
40	2
60	3
79	4
98	5
114	6
134	7
140	8
160	9
193	10
215	12
271	13
284	14
297	15

Time from start of rain (minutes)	Depth from surface to wetting front (inches)
Plot 68057196	
29	2
52	3
62	4
90	5
96	6
112	7
120	8
136	9
165	10
177	11
189	12
208	13
212	14
126	15
Plot 68098Y97	
47	2
91	3
116	4
167	5
206	6
260	7
277	8
312	9
347	10
374	11
Plot 68127F07	
28	2
34	3
44	4
55	5
91	7
97	8
133	9
159	10
184	11
197	12
243	13

TABLE A III. SATURATION AND DEPTH FROM SOIL SURFACE DATA AT DIFFERENT TIMES OBTAINED FROM INFILTRATION PLOTS.

Depth (inches)	Saturation (percent)					
	0 min.	48 min.	100 min.	150 min.	202 min.	240 min.
Plot 68057196						
2	7	45	50	52	58	56
4	18	29	75	77	80	81
6	27	50	61	74	73	69
8	31	12	11	50	64	66
10	46	46	46	61	94	91
12	43	43	43	43	63	76
15	34	34	34	34	35	82
18	36	36	36	36	36	46
21	28	28	28	28	28	36
24	24	29	29	29	29	28

Depth (inches)	Saturation (percent)				
	0 min.	30 min.	60 min.	110 min.	180 min.
Plot 68057396					
2	42	60	63	63	63
4	46	49	72	75	74
6	53	53	72	79	80
8	60	60	68	82	82
10	62	62	62	79	79
12	63	63	63	82	90
15	54	54	54	54	74
18	59	59	59	59	77
21	58	58	58	58	66
24	51	51	51	51	45

TABLE A III. (CONTINUED).

Depth (inches)	Saturation (percent)					
	0 min.	47 min.	110 min.	176 min.	228 min.	300 min.
Plot 68127D07						
2	15	32	62	68	67	71
4	19	22	51	69	75	75
6	14	14	18	43	61	74
8	50	51	56	61	71	85
10	41	41	41	52	71	78
12	44	44	44	44	53	64
15	39	39	39	39	43	57
18	39	39	39	39	39	45
21	42	42	42	42	42	42
24	42	42	42	42	43	43

Depth (inches)	Saturation (percent)					
	0 min.	30 min.	95 min.	165 min.	230 min.	270 min.
Plot 68127F07						
2	16	23	59	77	82	83
4	20	24	49	76	73	74
6	14	14	23	37	52	75
8	28	32	46	55	58	61
10	33	33	33	39	60	86
12	39	39	39	43	63	75
15	31	31	31	31	42	64
18	60	60	60	60	60	72
21	46	46	46	46	46	50
24	56	56	56	56	56	58

TABLE A III. (CONTINUED).

Depth (inches)	Saturation (percent)						
	0 min.	100 min.	205 min.	302 min.	405 min.	510 min.	581 min.
Plot 68098Z97							
2	12	65	69	72	73	73	77
4	15	19	55	72	72	75	77
6	27	27	44	56	71	78	90
8	39	38	40	47	74	85	82
10	37	37	37	37	47	63	63
12	47	47	47	47	56	58	71
15	51	51	51	51	51	51	61
18	49	49	49	49	49	49	55
21	50	59	59	59	59	59	53
24	53	53	53	53	53	53	70

Depth (inches)	Saturation (percent)					
	0 min.	74 min.	150 min.	220 min.	305 min.	377 min.
Plot 68098Y97						
2	12	47	70	77	81	77
4	14	13	38	69	73	75
6	25	25	27	32	69	69
8	34	34	34	34	61	78
10	49	49	49	49	56	62
12	39	39	39	39	42	40
15	42	42	42	42	42	42
18	54	54	54	54	54	54
21	50	50	50	50	50	50
24	46	46	46	46	46	46

TABLE A IV. TIME AND INFILTRATION RATE DATA OBTAINED FROM INFILTRATION PLOTS.

Time from start of rain (minutes)	Infiltration rate (inches/hour)				
	Plot 196	Plot 396	Plot Y97	Plot Z97	Plot F07*
6	2.00				3.00
8	1.15			2.00	2.90
10	0.80		2.50	1.60	2.90
12	0.60	2.00	2.05	1.70	2.90
14	0.50	1.45	2.00	1.65	2.95
16	0.35	1.30	1.95	1.50	2.95
18	0.40	1.35	1.80	1.55	2.90
20	0.35	1.35	1.65	1.60	2.90
22	0.30	1.30	1.80	1.50	2.90
24	0.35	1.20	1.65	1.40	2.85
26	0.30	1.20	1.50	1.40	2.80
28	0.20	1.20	1.50	1.40	2.75
30	0.15	1.15	1.50	1.35	2.70
32	0.30	1.15	1.60	1.30	2.70
34	0.40	1.15	1.40	1.35	2.50
36	0.15	1.30	1.30	1.30	2.35
38	0.30	1.25	1.25	1.25	2.35
40	0.45	1.20	1.15	1.30	2.20
42	0.40	1.30	1.05	1.35	2.10
44	0.50	1.30	1.00	1.35	2.05
46	0.30	1.30	1.10	1.25	1.95
48	0.30	1.20	1.00	1.25	1.85
50	0.35	1.15	1.00	1.25	1.70
52	0.20	1.15	1.00	1.25	1.55
54	0.25	1.00	0.70	1.35	1.60
56	0.15	1.00	0.80	1.35	1.60
58	0.05	1.10	1.00	1.25	1.50
60	0.20	1.00	0.90	1.20	1.50
62	0.30	1.00	1.00	1.25	1.40
64	0.30	1.00	1.00	1.25	1.30
66	0.35	1.05	0.85	1.15	1.30
68	0.20	1.05	0.80	1.20	1.35
70	0.05	0.85	0.85	1.25	1.30
72	0.15	0.65	0.85	1.30	1.25
74	0.20	0.70	0.80	1.35	1.25
76	0.20	0.95	0.65	1.25	1.25
78	0.40	0.90	0.70	1.25	1.25
80	0.60	0.90	0.90	1.15	1.20
82	0.50	0.90	0.85	1.15	1.15
84	0.20	0.80	0.90	1.20	1.10
86	0.15	0.85	0.90	1.15	1.15
88	0.30	0.95	0.65	1.15	1.15
90	0.30	0.95	0.70	1.15	1.05

TABLE A IV. (CONTINUED).

Time from start of rain (minutes)	Infiltration rate (inches/hour)				
	Plot 196	Plot 396	Plot Y97	Plot Z97	Plot F07
92	0.30	0.90	0.95	1.10	1.05
94	0.30	0.95	0.85	1.15	1.15
96	0.30	1.00	0.75	1.20	1.15
98	0.35	1.00	0.85	1.05	1.10
100	0.45	1.00	0.80	1.05	1.10
102	0.35	1.00	0.85	1.10	1.10
104	0.20	0.90	0.90	1.10	1.10
106	0.20	0.70	0.80	1.10	1.15
108	0.30	0.65	0.85	1.10	1.15
110	0.35	0.75	0.85	1.15	1.10
112	0.35	0.85	0.80	1.10	1.10
114	0.45	0.85	0.60	1.05	1.10
116	0.45	0.80	0.65	1.15	1.10
118	0.35	0.70	0.70	1.10	1.10
120	0.25	0.85	0.75	1.00	1.10
122	0.25	1.00	0.90	0.95	1.10
124	0.25	0.80	0.65	0.90	1.10
126	0.15	0.70	0.55	1.00	1.10
128	0.45	0.80	0.80	1.10	1.10
130	0.50	0.85	0.95	1.05	1.05
132	0.20	0.80	0.56	1.05	1.05
134	0.35	0.80		1.00	1.10
136	0.50	0.80		0.80	1.10
138					1.10
140					1.10
142					1.05
144					1.05
146					1.05
148					1.00
150					1.00
152					1.05
154					1.10
156					1.05
158					1.05
160					1.10
162					1.05
164					1.05
166					1.05
168					1.00
170					0.95
172					0.90
174					0.90
176					0.95

TABLE A IV. (CONTINUED).

Time from start of rain (minutes)	Infiltration rate (inches/hour)				
	Plot 196	Plot 396	Plot Y97	Plot Z97	Plot F07
178					1.05
180					1.13
182					1.20

*F07 time starts at 5 minutes instead of 6 minutes and stays 1 minute fast throughout the list.

TABLE A V. SATURATION AND CAPILLARY PRESSURE HEAD DATA FOR SURFACE DEPTH SOIL CORES OBTAINED FROM INFILTRATION PLOTS.

Drainage		Imbibition	
P_c (Cm H_2O)	Sat ($\frac{cm^3}{cm^3}$)	P_c (Cm H_2O)	Sat ($\frac{cm^3}{cm^3}$)
Plot 68057196			
3.7	0.97	432.0	0.41
14.0	0.94	260.0	0.49
32.2	0.90	200.0	0.52
42.7	0.87	162.0	0.56
53.5	0.84	131.0	0.59
63.5	0.80	109.0	0.62
72.5	0.76	86.0	0.66
		58.0	0.69
		34.0	0.74
		17.5	0.79
		8.6	0.84
		4.0	0.88
		0.0	1.00
Plot 68057396			
3.5	0.98	545.0	0.25
9.3	0.96	499.0	0.29
11.4	0.94	371.0	0.34
24.1	0.89	150.0	0.43
32.9	0.85	39.6	0.52
57.7	0.77	20.0	0.56
84.8	0.73	11.0	0.61
110.0	0.68	5.5	0.65
163.0	0.64	0.0	0.76
224.0	0.59		
515.0	0.50		
Plot 68098Z97			
1.6	0.98	432.0	0.71
25.9	0.95	243.0	0.76
71.8	0.93	145.0	0.82
107.0	0.92	71.0	0.88
126.0	0.91	25.0	0.94
223.6	0.86	7.7	1.00
340.0	0.81	0.0	1.00
458.0	0.77		

TABLE A V. (CONTINUED).

Drainage		Imbibition	
P_c (Cm H_2O)	Sat ($\frac{cm^3}{cm^3}$)	P_c (Cm H_2O)	Sat ($\frac{cm^3}{cm^3}$)
Plot 68127D07			
6.9	0.98	556.0	0.36
38.2	0.95	318.0	0.45
79.0	0.93	225.0	0.50
121.0	0.91	163.0	0.54
112.0	0.89	121.0	0.59
171.0	0.86	80.0	0.64
228.0	0.82	43.3	0.68
299.0	0.77	21.5	0.73
514.0	0.66	8.1	0.77
		3.7	0.82
		0.0	0.88
Plot 68127F07			
0.8	0.98	411.0	0.48
1.8	0.97	280.0	0.52
7.2	0.94	142.0	0.56
16.7	0.91	106.0	0.58
41.5	0.87	50.0	0.62
48.3	0.84	19.5	0.66
73.8	0.81	5.1	0.70
115.0	0.78	0.0	0.78
160.0	8.75		
205.0	0.71		
374.0	0.61		

TABLE A VI. SATURATION AND CAPILLARY PRESSURE HEAD DATA FOR SOIL CORES OBTAINED FROM INFILTRATION PLOTS.

Drainage	Saturation			Imbibition	Saturation		
P_c(Cm H_2O)	5.1 cm	10.2 cm	20.3 cm	P_c(Cm H_2O)	5.1 cm	10.2 cm	20.3 cm
Plot 68057196							
1.52	0.697	0.838	0.729	1.52	0.754	0.777	0.653
5.08	0.690	0.831	0.713	7.62	0.707	0.698	0.560
10.16	0.677	0.809	0.674	15.24	0.673	0.653	0.515
15.24	0.666	0.771	0.621	25.40	0.644	0.613	0.480
20.32	0.666	0.756	0.598	38.10	0.619	0.576	0.452
30.48	0.660	0.688	0.552	50.80	0.597	0.547	0.432
45.72	0.644	0.626	0.499	63.50	0.580	0.524	0.414
66.04	0.579	0.574	0.450	76.20	0.564	0.508	0.400
86.36	0.563	0.540	0.420	101.60	0.547	0.487	0.384
106.68	0.554	0.514	0.400	152.40	0.533	0.470	0.371
152.40	0.533	0.470	0.371				
Plot 68057396							
1.52	0.887	1.022	0.960	1.524	0.767	0.842	0.752
5.08	0.854	0.925	0.908	15.24	0.695	0.764	0.632
10.16	0.827	0.897	0.856	30.48	0.644	0.712	0.570
20.32	0.776	0.844	0.747	50.80	0.593	0.657	0.512
30.48	0.732	0.793	0.673	76.20	0.542	0.610	0.458
40.64	0.690	0.749	0.621	101.60	0.503	0.576	0.422
50.80	0.658	0.713	0.580	152.40	0.467	0.545	0.389
71.12	0.610	0.665	0.525	213.36	0.448	0.528	0.374
101.60	0.560	0.619	0.475				
152.40	0.499	0.568	0.414				
213.36	0.448	0.528	0.374				
Plot 68127D07							
1.524	0.752	0.880	0.906	1.524	0.455	0.743	0.722
7.62	0.500	0.756	0.775	10.16	0.374	0.636	0.614
15.24	0.441	0.683	0.676	20.32	0.343	0.592	0.560
25.40	0.400	0.628	0.603	35.56	0.306	0.551	0.488
35.56	0.375	0.589	0.556	50.80	0.287	0.522	0.449
50.80	0.349	0.548	0.512	76.20	0.270	0.490	0.419
76.20	0.315	0.504	0.460	102.108	0.261	0.461	0.403
101.60	0.293	0.479	0.432	152.40	0.251	0.439	0.392
152.40	0.251	0.444	0.392	213.36	0.191	0.416	0.350
213.36	0.191	0.416	0.350				

TABLE A VI. (CONTINUED).

Drainage	Saturation		Imbibition	Saturation	
P_c(Cm H_2O)	5.1 cm	10.2 cm 20.3 cm	P_c(Cm H_2O)	5.1 cm	10.2 cm 20.3 cm
Plot 68098Y97					
5.08		0.849 0.901	1.52		0.863 0.837
7.62		0.847 0.883	5.08		0.823 0.760
10.16		0.848 0.820	12.70		0.782 0.675
12.70		0.847 0.788	17.78		0.757 0.637
15.24		0.844 0.752	25.40		0.730 0.597
17.78		0.841 0.710	38.10		0.699 0.557
20.32		0.800 0.678	50.80		0.673 0.527
27.94		0.778 0.634	76.20		0.637 0.495
33.02		0.757 0.604	101.60		0.617 0.477
40.64		0.726 0.574	152.40		0.598 0.458
55.88		0.681 0.538			
76.20		0.652 0.511			
101.60		0.625 0.485			
127.00		0.610 0.471			
152.40		0.598 0.458			
Plot 68098Z97					
1.27		0.819 0.853	1.016	0.813	0.736 0.771
3.81		0.819 0.824	3.810	0.793	0.710 0.746
5.08		0.817 0.822	6.858	0.776	0.692 0.730
7.62		0.806 0.807	8.89	0.764	0.679 0.719
10.16		0.794 0.796	10.16	0.749	0.663 0.704
15.24		0.739 0.767	12.70	0.734	0.648 0.691
17.78		0.722 0.759	17.78	0.716	0.629 0.677
22.86		0.704 0.747	22.86	0.701	0.611 0.663
27.94	0.793	0.683 0.732	27.94	0.687	0.595 0.650
38.10	0.750	0.634 0.701	38.10	0.664	0.567 0.631
45.72	0.721	0.606 0.683	55.88	0.638	0.534 0.606
55.88	0.691	0.579 0.661	76.20	0.619	0.511 0.586
76.20	0.655	0.545 0.627	101.60	0.605	0.492 0.571
101.60	0.627	0.516 0.596	149.86	0.594	0.482 0.560
149.86	0.594	0.482 0.560			

APPENDIX B

Soil Descriptions

SOIL DESCRIPTIONS[1]

Soil Descriptions from the Lake Bed Site on Reynolds Creek Watershed

Soil Name - Nannyton loam.

Classification - Fine-loamy, mixed, mesic family of Typic Haplargids.

Location - At rainfall simulator test site #057496, Lakebed Flats (Plots 196, 396).

Natural Vegetation - Shadscale, big sagebrush, cheatgrass and peppergrass.

Climate - Approximately eight inches mean annual precipitation with dry summers; mesic temperature regime.

Parent Material - Lacustrine and possibly some alluvial material.

Physiography - Dissected old lake terrace.

Relief - Undulating.

Slope - Two to three percent, northwest facing.

Drainage - Well-drained.

Ground Water - Deep, probably more than 20 feet.

Elevation - About 3,500 feet.

Stoniness - None or slight.

Moisture - Soil is moist throughout because of water added by the rainfall simulator.

Erosion - Slight.

Permeability - Moderate.

---

[1]Soil descriptions taken from U.S. Soil Survey Staff. Soil Survey Manual, U.S. Department of Agriculture Handbook, No. 18, pg. 503, 1962.

Additional Notes - Profile was described between the scanning tubes from the rainfall simulator. There are many fine flakes of mica throughout the profile.

Profile Description - (Colors are for dry soil unless noted otherwise.)

A21 - 0-2 inches - Pale brown (10YR 6/3); slightly gravelly sandy loam; dark grayish brown (10YR 4/2) moist; moderate, thin, platy, parting to weak fine granular structure; soft, very friable, nonsticky, nonplastic; common fine and few medium roots; many fine and medium vesicular pores; noncalcareous; clear smooth boundary.

A22 - 2-5 inches - Light gray (10YR 7/2) gritty loam; dark brown (10YR 4/3) moist; weak, thin, platy, parting to weak fine granular structure; soft, friable, nonsticky, slightly plastic; common fine and medium roots; many fine vesicular pores; noncalcareous; gradual smooth boundary.

A3 - 5-8 inches - Very pale brown (10YR 7/3); slightly gravelly loam with fine gravel; dark brown (10YR 4/3) moist; weak, thin platy parting to weak fine subangular blocky structure; slightly hard, friable, nonsticky, slightly plastic; common fine, few medium roots; common fine vesicular and tubular pores; noncalcareous; clear smooth boundary.

B21t - 8-12 inches - Pale brown (10YR 6/3) light clay loam; brown (10YR 4/3) moist; weak, coarse, prismatic, parting to moderate, fine and medium subangular blocky structure; hard, firm, plastic and sticky; few fine and medium roots; many fine tubular pores; thin, nearly continuous clay films;

noncalcareous; abrupt and smooth boundary.

B22t - 12-15 inches - Very pale brown (10YR 7/3) gravelly clay loam; brown (10YR 4/3) moist; moderate, fine, subangular blocky structure; hard, firm, sticky, and plastic; few fine and medium roots; common fine and medium tubular pores; thin, nearly continuous clay films; noncalcareous; abrupt and smooth boundary.

C1ca - 15-19 inches - Very pale brown (10YR 7/3) gritty loam; dark yellowish brown (10YR 4/4) moist; weak, fine subangular blocky structure; soft, friable, nonsticky, nonplastic; few fine roots; few fine tubular pores; highly calcareous; many lime veins; clear wavy boundary.

Soil Descriptions from the Lower Sheep Creek Site on Reynolds Creek Watershed

Soil Name - Searla gravelly loam.

Location - Sheep Creek Study Basin; in tall sage SE of basin. (Plots F07, D07).

Vegetation and Land Use - Range; big sage.

Topography - Alluvial fan.

Drainage - Well drained.

Parent Material - Alluvium or colluvium from rhyolite.

Horizon	Description
A11	0 - 2-1/2 inches: gravelly loam; weak to moderate platy breaking to very fine granular structure.
A12	2-1/2 - 6 inches: gravelly heavy loam; moderate to strong platy breaking to fine granular structure; plentiful fine roots.
B11t	6 - 13 inches: light clay loam; weak to moderate subangular blocky structure; plentiful fine roots; weak to medium patchy clay films.
B12t	13 - 22 inches: gravelly clay loam; moderate to strong subangular blocky structure; few fine roots; weak to medium nearly continuous clay films.

Soil Descriptions from the Nancy's Gulch Site on the Reynolds Creek Watershed

Soil Name - Babbington loam.

Classification - Fine-loamy, mixed, mesic family of Aridic Calcic Argixerolls

Location - Near the southeast corner of the Nancy exclosure (Plots Y97, Z97).

Natural Vegetation - Big sagebrush, bluebunch wheatgrass, squirrel tail, Sandberg bluegrass.

Climate - Eleven to twelve inches mean annual precipitation; mesic, but marginal to frigid temperature regime.

Parent Material - Residuum from basalt, possibly some loess in the surface horizons.

Physiography - Dissected basalt plateau.

Relief - Gently rolling.

Slope - Four percent, east facing.

Elevation - About 4,400 feet.

Drainage - Well drained; ground water very deep.

Stoniness - Few surface stones and some stones throughout the profile.

Moisture - Soil is dry to six inches; slightly moist six to twenty inches; and dry below twenty inches.

Erosion - Moderate.

Permeability - Moderately slow.

Profile Description - (Colors are for dry soil unless noted otherwise.)

A1 - 0-3 inches - Brown (10YR 5/3) loam; very dark grayish brown (10YR 3/2) moist; weak, coarse, platy; parting to weak fine

granular structure; slightly hard, very friable, slightly sticky, slightly plastic; many fine few medium and coarse roots; many fine and medium pores; noncalcareous; clear smooth boundary.

B1 - 3-6 inches - Pale brown (10YR) slightly gravelly heavy loam; dark brown (10YR 3/3) moist; weak thin platy, parting to moderate very fine subangular blocky structure; slightly hard, friable, slightly plastic, many fine few medium and coarse roots; many fine interstitial pores; noncalcareous; clear smooth boundary.

B21t - 6-12 inches - Brown (10YR 5/3) clay loam; dark brown (10YR 3/3) moist; strong fine subangular blocky structure; hard, firm, sticky, plastic; common fine few medium and coarse roots; many fine and medium interstitial and tubular pores; thin nearly continuous clay films; noncalcareous; gradual smooth boundary.

B22t - 12-20 inches - Yellowish brown (10YR 5/4) slightly gravelly heavy clay loam; dark brown (10YR 3/3) moist; weak medium prismatic parting to moderate fine subanular blocky structure; hard, firm, sticky, plastic; common fine few medium and coarse roots; common fine few medium tubular pores; thin continuous clay film; noncalcareous; clear smooth boundary.

B3ca - 20-28 inches - Light yellowish brown (10YR 6/4) gravelly clay loam; dark yellowish brown (10YR 4/4) moist; moderate medium and fine subangular blocky structure; hard, firm,

sticky, and plastic; few fine and medium roots; common fine tubular pores; thin nearly continuous clay films; moderately calcareous with common lime veins that are highly calcareous; clear smooth boundary.